NATURAL PRODUCT DERIVATIVE ACTIVATES AUTOPHAGY IN CANCER CELLS

Thesis by

URSULA-CLAIRE ANDONG KOUNG EDZIDZI

Supervisor A/Prof. Denver Hendricks

In the Fulfillment of the Requirements for the degree of Masters of Science (Medical Biochemistry)

University of Cape Town

Cape Town, South Africa

August 2016

DECLARATION

I, **URSULA-CLAIRE ANDONG-KOUNG-EDZIDZI** hereby declare that the work on which this dissertation/thesis is based is my original work (except where acknowledgements indicate otherwise) and that neither the whole work nor any part of it has been, is being, or is to be submitted for another degree in this or any other university.

I empower the university to reproduce for the purpose of research either the whole or any portion of the contents in any manner whatsoever.

Signature: Signed by candidate

Date: 21.10.2016

ACKNOWLEDGMENTS

I would like to express my gratitude to the following people:

To God for giving me the strength and blessing me with peace to carry on with this project.

My supervisors, A/prof Denver T. Hendricks, for his expertise, excellent supervision and constant advice, love and support.

Dr Kate Hadley, for her expertise and excellent ideas for this project.

A/prof Virna Leaner for her support and ideas.

My parents, brothers and sister for their tremendous support and love.

Members of the cancer Research Group: Mateen Wagiet, Aderonke Ajayi-Smith, Erin Strydom, Cherise Dunn, Alicia Chi, Tamara Sweet, Sarah Carden and Pauline van der Watt for their help in the laboratory. I will miss our jokes and stories.

Hajira Guzgay and Robert Samuels, for their excellent management of the laboratory and the people within it.

Agence National des Bourses et Stages for financial assistance.

TABLE OF CONTENTS

ABBREVIATIONS

AKT	AK (mouse strain) Thymoma
AMPK	AMP-activated protein kinase
ATF6	Activating transcription factor 6
ATG	Autophagy-related-genes
ATP	Adenosine triphosphate
Bad	Bcl-2 agonist of cell death
Bak	Bcl-2 agonist killer 1
Bax	Bcl-2-associated x protein
BC	Before Christ
BCA	Bicinchoninic acid
Bcl-2	B-cell lymphoma 2
Bif 1	Bax-interacting factor 1
Bik	Bcl-2-interacting killer
Bim	Bcl-2-interacting mediator of cell death
BSA	Bovine serum albumin
CaMKKβ	Calcium-activated calmodulin-dependent kinase kinase-beta
CDK	Cyclin dependent kinase
CHOP	C/EBP homologous protein
CI	Confidence intervals
CMA	Chaperone-mediated autophagy
CNS	Central nervous system
COX-2	Cyclooxygenase-2
C_T	Cycle threshold

DEPC	Diethylpyrocarbonate
DHA	Dihydroartemisinin
DMEM	Dulbecco's Modified Eagle Medium
DMSO	Dimethyl sulphoxide
DNA	Deoxyribonucleic acid
EDTA	Ethylene diamine tetra acetic acid
eIF2α	eukaryotic initiation factor 2 alpha
ER	Endoplasmic reticulum
FBS	Foetal bovine serum
FDA	Food drug administration
FIP200	The focal adhesion kinase family-interacting protein of 200
GAPDH	Glyceraldehyde-3-phosphate dehydrogenase
GLOBOCAN	Global burden of cancer
GαM	Goat anti-mouse
GαR	Goat anti-rabbit
GusB	*β-glucoronidase*
HIV/AIDS	Human immunodeficiency virus/acquired immunodeficiency syndrome
hVps34	Human Vacuolar protein sorting 34
IARC	International Agency for Research on Cancer
IRE1	Inositol requiring enzyme 1
JNK	c-jun-N-terminal Kinase
kDa	KiloDaltons
LAMP	Lysosome-associated membrane protein
LC3	Microtubule-associated protein 1 light chain 3

3-MA	3-Methyladenine
MMP9	Metalloproteinase9
mLST8	mammalian lethal with sec-thirteen protein 8
mRNA	Messenger ribonucleic acid
mTOR	Mammalian target of Rapamycin
MTT	3-[4,5-dimethylthiazol-2-yl]-2,5-diphenyltetrazolium bromide
µg	Microgram
µl	Microlitre
µM	Micromolar
NA	Not Active
NCDs	Non-communicable diseases
NCI	National Cancer Institute
NFκB	Nuclear factor kappa-light-chain-enhancer of activated B cells
Noxa	Phorbol-12-myristate-13-acetate-induced protein 1
PARP	Poly (ADP-ribose) polymerase
PBS	Phosphate buffered saline
PCD	Programmed cell death
PE	Phosphatidylethanolamine
PERK	Protein Kinase R-like ER Kinase
PI3K	Phosphatidylinositol 3-kinase
PIP	Phosphatidylinositol-phosphate
PIP_2	Phosphatidylinositol 4,5-biphosphate
PIP_3	Phosphatidylinositol -3,4,5-triphosphate
pJNK	Phophorylated JNK

PRAS40	Proline rich AKT substrate of 40kDa
PTEN	Phosphatase and tension homolog deleted on chromosome 10
PUMA	P-53 up-regulated modulator of apoptosis
RAPTOR	Regulatory associated protein of mTOR
Rheb	Ras Homolog Enriched in Brain
RNA	Ribonucleic acid
ROS	Reactive oxygen species
RT-PCR	Reverse transcription polymerase chain reaction
SDS	Sodium dodecyl sulphate-polyacrylamide gel electrophoresis
SiRNA	Small interfering RNA
SP	SP600125
TBS-T	Tris buffered saline with 0.1 % Tween-20
TCTP	Translationally controlled tumor protein
TEMED	N, N, N-Tetramethyl-ethylene diamine
TEMPOL	4-hydroxy-2, 2,6,6-tetra-ethylpiperidine 1-oxyl
TNF	Tumour necrosis factor
TRAIL	TNF-related apoptosis-inducing ligand
TSC	Tumour sclerosis complex
ULK1 and 2	Unc-51-like kinase 1 and 2
UPR	Unfolded Protein Response
UVRAG	Ultraviolet irradiation resistant-associated gene
Vps	Vacuolar protein sorting
VEGF	Vascular endothelial growth factor
WHO	World Health Organization

ABSTRACT

Artemisinin, a natural product and its derivatives are potent antimalarial compounds, which have shown anticancer activity. In this study, we further characterized a novel artemisinin derivative namely EXP57EA which was previously designed and synthesized by the Chemistry Department at the University Of Cape Town. We determined the effect of EXP57EA on a panel of cancer cell lines, characterized the mode of cell death and also performed preliminary investigations of the signaling pathways that trigger the mode of cell death.

Dihydroartemisinin (DHA), EXP57EA and cisplatin were screened on a selected panel of cancer cell lines: 3 esophageal cancer cell lines WHCO1, WHCO5, KYSE150; one breast cancer cell line MDA-MB-231 and one cervical cancer cell line SiHa. The 3-[4, 5-dimethylthiazol-2-yl]-2, 5-diphenyltetrazolium bromide (MTT) assay, and analysis with GraphPad prism software were used to calculate IC_{50} values. EXP57EA displayed toxicity in the panel of cancer cell lines studied, and had lower IC_{50} values (IC_{50} values were ranging from 15.8 μM to 25.1 μM) than DHA and cisplatin. DHA was only active in two cells lines: WHCO1 (21.3 μM) and WHCO5 (77.3 μM), IC_{50} values of cisplatin were ranging from 31.2 μM to 108.1 μM. EXP57EA was further investigated to understand the mode of cell death activated in the panel of cancer cell lines.

The results showed that EXP57EA did not induce apoptosis in any of the cell lines studied, whereas DHA induced apoptosis, based on the PARP cleavage assay. In contrast, treatment with EXP57EA induced the appearance of vacuoles in treated cells compared to untreated cells, which was suggestive of autophagy. Autophagy was monitored by analyzing the expression level of two autophagy markers, Beclin1 and LC3-II by western blot. It was observed that EXP57EA treatment caused changes in the expression levels of both Beclin1 and LC3-II. We showed that EXP57EA induced elevated levels of autophagy, based on an increase in the flux of

autophagy in the treated cells, since the lysosomal inhibitors ammonium chloride (NH_4Cl) and chloroquine substantially blocked LC3-II turnover in WHCO1 (confirmed previous result in our laboratory) and SiHa cancer cell lines.

Furthermore, we also showed that treatment with EXP57EA resulted in increased expression of CHOP (by Real-Time PCR), and activated the PERK/eIF2α pathway, since treatment of WHCO1 cells with EXP57EA stimulated phosphorylation of eIF2α, suggesting that ER stress might be involved in mediating EXP57EA-induced cell death. Our results also suggested that EXP57EA activated the JNK pathway since treatment of WHCO1 and WHCO5 cells with EXP57EA stimulated phosphorylation of c-jun and resulted in elevated levels of total c-jun. These results suggested the JNK pathway might also be involved in EXP57EA-induced cell death. However, the proposed involvement of the PERK/eIF2α pathway and the JNK pathway in EXP57EA-mediated autophagy is of a preliminary nature, and further work will have to be done to confirm the involvement of these pathways.

This study showed that EXP57EA may have potential as an anticancer drug lead.

CHAPTER 1:

LITERATURE REVIEW

1.1 Cancer: A global health problem

Non-communicable diseases (NCDs) constitute a major health crisis worldwide illustrated by the high prevalence of diseases such as cardiovascular disease, cancer, stroke and diabetes (Beaglehole et al. 2011). It was reported that the incidence of cancer surpassed AIDS/HIV, tuberculosis and malaria (Moten et al. 2014). Based on estimates, there were 12.4 million estimated new cancer cases and 7.6 million cancer-related deaths in low and middle-income countries in 2008 (Ferlay *et al*., 2012). In 2012, approximately 14 million new cancer cases were reported, and this figure is anticipated to increase over the next twenty years (WHO, 2014). With the number of cancer-related deaths predicted to increase substantially due to the adoption of a lifestyle that is prone to cancer, namely physical inactivity, excess smoking and unhealthy diet (Parkin et al. 2002; McCormack & Schüz 2012), it is necessary to increase our effort to fight this disease. This project will focus on exploring natural product derivatives as a source of compounds that may have activity against cancer cells, and could be developed into chemotherapeutic agents. There are a number of options open to address the burden of cancer that confronts us: (1) prevention by reducing the exposure of individuals to risk factors associated with cancer such as tobacco, physical inactivity, infection with viruses such as hepatitis B or C, overweight and obesity, alcohol consumption, ionizing radiation from natural, industrial and medical sources (Parkin et al. 2002); (Darby et al.

2005) (2) it is well known that diagnosing cancers at an early stage of the disease provides patients with the best possible chance of survival (Berry et al. 2005; Siegel et al. 2015) (3) medical treatment varies from surgical excision, chemotherapy and radiotherapy. The exact treatment regime and combination thereof depend on the type of cancer and stage of the disease (Siegel et al. 2015; Freedman et al. 2012; Machiels et al. 2014).

1.2 Natural products as a source of novel chemotherapeutic drug leads

The use of plants as medicinal treatments started thousands years ago and the first records come from Mesopotamia. Those reports record the widespread use of up to 1000 plants extracts for the treatment of various ailments (Tobin et al. 2012).

Natural products and compounds isolated from plants have been considered as prototypes or leads in drug development and their molecular modifications have resulted in compounds with remarkable therapeutic possibilities (Gordaliza 2007). Furthermore, natural products have served an important source for anticancer drug development, with approximately 55 % of small-molecule anticancer agents derived from plants and other types of organisms, including terrestrial microbes and marine organisms (Newman & Cragg 2016). As described below, plant-derived natural products and their derivatives have yielded a number of well-known chemotherapeutic agents still in use today.

In 1880, the isolation of podophyllotoxin from *podophyllum peltatum* (Rosenthal & Meshnickb 1996) was reported. However, it was only in 1950 that the correct structure of this compound was published (Nirmala et al. 2011). Many podophyllotoxin ligands were isolated and introduced into clinical trials but failed due to efficacy and toxicity limitations (Prakash et al. 2013). However, through extensive research, two active agents (derived from an analog 4'-dimethylepipodophyllotoxin) namely teniposide and etoposide

were developed and are currently clinically used in the treatment of various cancers including lymphomas, bronchial, small-lung, leukeamia and testicular cancers (Takahashi et al. 2005). Podophyllotoxin prevents the polymerization of tubulin into microtubules whereas the analog inhibits topoisomerase II, thus preventing the cleavage and resealing of DNA strands (Newman et al. 2000).

The Vinca alkaloids Vinblastine and Vincristine were isolated from the Madagascan herb *Catharantus roseus*. A crude extract of this plant was investigated in the laboratory for it antidiabetic potential using experimental animals, and the antileukemic activity of that crude extract was discovered by serendipity (Newman et al. 2000). Vinblastine is active against testicular, lymphoma, breast, head and neck, cervico-uterine and bladder cancers, whereas, Vincristine was found to be active against pediatric tumors, Hodgkin's disease and also non-Hodgkin lymphoma. These drugs, like podophyllotoxin inhibit mitosis by binding to tubulin to prevent their polymerization into microtubules (Bhanot. et al. 2011).

The successful use of podophyllotoxin and the discovery of the Vinca alkaloids highlighted the value of plants as potential sources of drug leads for cancer therapy, and triggered a wave of exploration and research into natural products. As part of this process, the Pacific Yew tree was one of many plants investigated and Paclitaxel (Taxol) was discovered (Cragg et al. 1993). The US FDA approved Taxol in 1992 for the treatment of metastatic ovarian cancer, with promising clinical trials observed for the treatment of breast, lung and head and neck cancers (Yue-Zhong Shu 1998). Docetaxel, a semisynthetic analog of paclitaxel, was found to be more potent due to better water solubility. This compound can be used in cancer patients resistant to paclitaxel and is active against locally metastatic breast and non-small lung cancers (Fang & Liang 2005; Ojima et al. 2000). Paclitaxel and docetaxel also inhibit mitosis, however, they act as microtubule stabilizers, thus promoting their polymerization (Hait et al. 2007).

Camptothecin, isolated from *Camptotheca acuminate* (Cragg & Newman

2005) was subjected to clinical trials by the National Cancer Institute (NCI) in 1970 and withdrawn due to problems with water solubility and toxicity. To overcome these major drawbacks, the derivatives Irinotecan and Topotecan were developed and are used as second line treatment in various cancers (Fuchs et al. 2006). Topotecan is effective against ovarian and small cell lung cancers and Irinotecan is effective against colorectal cancer (Liu et al. 2006). Exatecan is a synthetic derivative of camptothecin. This compound has been shown to be more efficient against tumours with better solubility and less toxicity compared to the parental compound, camptothecin (Reichardt et al. 2007). Exatecan was shown to be active against various tumors *in vitro and in vivo*. Camptothecin derivatives function to inhibit Topoisomerase I, interfering with DNA replication and transcription (Srivastava et al. 2005).

In summary, natural products derived from plants currently play an important role in the development of drugs for the treatment of cancer. While the parental compounds isolated from plants may not be used directly as anticancer drugs, they can be used as leads for the development of novel compounds with substantially improved characteristics such as solubility and general toxicity. Among the promising compounds with activity against cancer is the natural-product derived antimalarial drug, artemisinin (Maria P. Crespo-Ortiz & Wei 2012).

1.2.1 Artemisinin and its derivatives

Quinghao is a Chinese medicinal herb commonly known as *Artemisia annua* or *sweet wormwood* (Maude et al. 2010). The use of this plant in the treatment of malaria was first reported around the second century. It was recommended to drink a mixture containing boiled quinghao for the treatment of fevers with sweating and jaundice. In 1967, the Chinese government initiated an extensive investigation into the antimalarial properties of quinghao, and reported the effectiveness of a crude extract in mice infected with *plasmodium berghei* (Hsu 2006). Other studies reported no toxicity when

rats, cats and dogs were given a high dose of this extract. In 1972, a colourless, needle-shaped crystal active ingredient of *quinghao* was isolated and three years later *quinghaosu* was chosen as the name of the new compound. The western name for *quinghaosu* was artemisinine, which changed to artemisinin a few years later (Maude et al. 2010).

Artemisinin is a terpene lactone, which consists of a 1, 2, 4-trioxane, ring structure and contains an endoperoxide bridge (C-O-O-C). Despite its success as an antimalarial drug, this compound shows some pharmacological limitations such as poor bioavailability, its solubility in water and oil is low, and finally the half-life of this compound is short, approximately 2.5 hours *in vivo* (Ashton et al. 1998). The development of semisynthetic and fully synthetic artemisinin-like endoperoxide compounds was attempted to alleviate these limitations (Das 2015). The first generation of semisynthetic artemisinin-like compounds includes the lipid soluble arteether and artemether and the water-soluble artesunate, which are frequently used in the treatment of different malarial parasites including the resistant forms (Haynes et al. 2002). The second generation of artemisinin-like compound includes artemisone with substantially improved characteristics such as a long half-life and low toxicity (Das 2015). All semisynthetic artemisinin are obtained from dihydroartemisinin (DHA), which has been reported to be the most potent active metabolite of artemisinin (Du et al. 2013). The fully synthetic artemisinin-like compounds such as trioxolanes and ozonides are synthesized retaining the endoperoxide bridge, which is essential for their activation and efficacy as an anti-malarial agent (Creek et al. 2008; Jefford 2007).

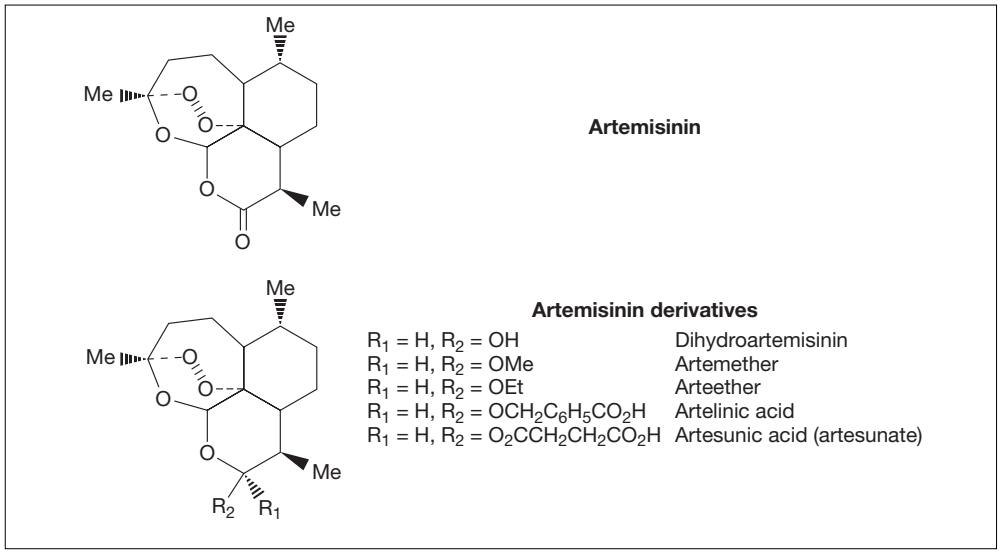

Figure 1.1: Structures of artemisinin and its first-generation (Dihydroartemisinin and Artesunate) and second-generation (Artemether, Arteether and Artelinic acid) derivatives (Firestone & Sundar 2009).

1.2.2 Artemisinin derivatives as potential chemotherapeutic agents

Numerous studies have investigated the anticancer effect of artemisinin and its semisynthetic derivatives *in vivo* and *in vitro* (Efferth et al. 2003). It has been reported that the proposed mechanism of action of Artemisinin is the iron-mediated cleavage of the endoperoxide bridge generating ROS and carbon-centered radical molecules that causes extensive protein damage and ultimately death of the malaria parasites, and presumably, cancer cells too (Maria P. Crespo-Ortiz & Wei 2012).

Woerdenbag and colleagues reported the first study on the cytotoxicity of artemisinins and its derivatives in 1993. In this study, artemisinin displayed activity in the micromolar range (29.8 μM) against Ehrlich ascites tumour (EAT) cells. However these cells were more susceptible to artemether, arteether, artesunate, artelinic acid and sodium artelinate with IC_{50} values between 12.2 μM and 19.9 μM (O'Neill et al. 2010; Woerdenbag et al., 1993). Further studies were conducted on the cytoxicity of these compounds on

HeLa S3 and Ehrlich ascites (EN19) cell lines and it was reported that artemisinin and its derivatives inhibited the growth of these tumour cells based on the results of the clonogenic assay (Beekman et al. 1996).

A study conducted by Efferth et al (2003) aiming at determining the effect of artesunate in 55 human cancer cell lines concluded that artesunate inhibits proliferation of leukemia, colon, melanoma, breast, prostate and Central Nervous System (CNS) cancer cell lines (Efferth et al. 2003). It has also been reported that DHA exerted its anticancer effects against pancreatic, lung and leukemic cancer cell lines (Lu et al. 2009). Furthermore, artemisone was showed to be more potent than artemisinin and able to successfully interact with other anticancer agents (Gravett et al. 2011).

Artemisinin has been shown to be effective against cancer by causing DNA damage or by interfering with different molecular signaling pathways involved in the disease of cancer. Du et al., 2010 demonstrated that the artemisinin derivative, artesunate induced DNA damage and membrane disruption in a pancreatic cancer xenograft mouse model *in vivo* (Du et al. 2010).

Artemisinin-like semisynthetic compounds are able to inhibit cancer cell growth by inhibiting signaling pathways involved in proliferation and by disrupting cell cycle checkpoints (Efferth et al. 2003; Das 2015). The most potent artemisinin-like compound, DHA showed arrest at G_2/M phase in pancreatic, osteosarcoma, leukemia and ovarian cancer cell line lines, while artesunate treatment interfered with G_2 in osteosarcoma, ovarian and A431 human epidermoid carcinoma cells (Gravett et al. 2011; Jiao et al. 2007). The growth arrest was associated with altered expression and activity of CDK2-4 and CDK2-6 responsible for the transition of G1 to S phase (Firestone & Sundar 2009; Johnson & Walker 1999).

The anticancer activity of artemisinin-derivatives has also been linked to the induction of apoptosis in cancer. Apoptosis is an extensively and well-

described process that is controlled by the Bcl2 genes family. The Bcl2 genes family includes the antiapoptotic *bcl-2 genes* and the proapoptotic genes Bax; Bad, Bim; Bik, Noxa and Puma that play a regulatory role in cancer through the mitochondria. Cell death through the intrinsic apoptosis pathway is achieved by an increase in the Bax/Bcl2 ratio, which results in release of mitochondrial cytochrome c and causes the activation of Caspases. It has been shown that artemisinin derivatives commonly induced rapid cell death via apoptosis through the disruption of the mitochondrial organelle, which then activates downstream events leading to cell death. Singh and Lai, (2004) reported that treatment of Leukemia cancer cells with DHA resulted in apoptosis after 1 hour (Singh & Lai 2004). DHA and artesunate treatments were shown to induce overexpression of the proapoptotic Bax, increased ratio of Bax/Bcl2, the release of cytochrome c and activation of caspases 9 and 3 resulting in osteosarcoma cell death. Activation of Caspase 8 and reduction in the expression of cyclin B1 and NF-KappaB was also observed. The extrinsic apoptotic pathway is mediated by the extracellular death ligands binding to various death receptors including death receptor 5 (DR5) to eliminate unwanted cells during development. A study done by He et al., 2010 reported that DHA treatment increased the expression of death receptor 5, which consequently resulted in apoptosis in different prostate cancer cell lines. Moreover, co-treatment with TRAIL enhanced the apoptotic effect of DHA by up to 35 % in the same cell line (He et al. 2010).

The role of the endoperoxide bridge of artemisinin and its derivatives has been extensively studied and reported to be pharmacologically important for their antimalarial effects (Das 2015). In the malarial parasite the activation of this bond is mediated through high concentrations of Ferrous iron, which consequently leads to the generation of free radicals (Bustos et al. 1994; Olliaro et al. 2001; Rosenthal & Meshnickb 1996). Interestingly, some cancer researchers have found that the anticancer effect of artemisinin and its derivatives has been also associated with the endoperoxide bridge (Mercer et al. 2007; Meunier et al. 2010). It was found that artemisinin compounds

without the endoperoxide bridge did not completely inhibit their anticancer effect. However, toxicity to cells was reduced compared to the compounds containing the trioxane ring structure (Maria P. Crespo-Ortiz & Wei 2012).

Iron ferrous and heme are important in the activation of artemisinin and its derivatives (Hamacher-Brady et al. 2011; Zhang & Gerhard 2009). It has been shown that the toxicity of these compounds was triggered by high influx of iron or iron-saturated holotransferrin, which then resulted in an increase of their anticancer activity up to 100 fold (Lai & Singh 1995; Lu et al. 2010; Lu et al. 2011; Mercer et al. 2011). Moreover, Lai et al. 2009 showed that conjugated artemisinin with an iron-carrying compound exhibited higher anticancer activity than artemisinin alone (Lai et al. 2009).

Anticancer drugs have certain properties such as high oxidative stress (ROS). Reactive oxygen species damage often occurs due to increased metabolic activity and the reduced expression levels of antioxidants in malignant cells (Pieniążek et al. 2013). Crespo-Ortiz et al. 2001 have suggested a possible scheme to explain the anti-cancer effects of artemisinins relating treatment of artemisinins to the generation of ROS and eventually activation of apoptosis (figure 1) (Bostwick et al. 2000; Mercer et al. 2007). Du et al. 2010 reported that microscopic analysis of cancer cells treated with artemisinin derivative namely artesunate showed early apoptotic subcellular changes by the activation of ROS (Du et al. 2010). Another study demonstrated that the generation of ROS preceded the toxicity of artesunate in the cervical Hela cancer cell line suggesting that ROS was the triggering factor (Zhou et al. 2012).

Factors such as calcium metabolism, endoplasmic reticulum stress (ER) and the binding calcium protein TCTP (translationally controlled tumour protein) can also regulate the anticancer effects of artemisinin (Noori & Hassan 2011; Stockwin et al. 2009). It has been found that the common IC_{50} value of

artesunate in a panel of cancer cell lines from the national cancer institute (NCI) correlated inversely with the microarray mRNA expression level of TCTP. Cancer cells expressing high levels of TCTP were found to be more sensitive to artesunate compared to those expressing low levels of TCTP. Even though the functional role of TCTP in the anticancer activity of artemisinin still needs to be investigated, the above-mentioned results suggest such a role (Baudet et al. 1998; Bommer & Thiele 2004).

Given that this project will explore cell death mechanisms activated by artemisinin and its derivatives, below, we discuss some of the different programmed cell death pathways that can be involved in cell death.

1.3 Programmed Cell death in cancer

One of the major processes controlling cell fate is programmed cell death. It is a genetically regulated process involved in development, homeostasis and removal of unwanted cells (Levine 2007; Hanahan & Weinberg 2011) and which has recently generated much interest because these processes typically represent the end-point of cancer treatment (Bialik et al. 2010; Tan et al. 2009). Three types of programmed cell death (PCD) are generally recognized: apoptosis (or PCD I), autophagy (or PCD II) and Necrosis (or PCD III).

Apoptosis or PCD I is the best characterized and reported cell death mechanism. PCD I plays an important role in quality control and repair processes by eliminating damaged, unwanted cells, which are critical for the development of various organisms (Hengartner 2000).

PCD II or autophagy is a catabolic process in eukaryotic cells involved in the removal of organelles and long-lived proteins. Moreover, autophagy plays a role in the quality control of organelles and proteins to enhance cell survival under starvation conditions (Klionsky 2005).

In contrast to apoptosis and autophagy which are energy dependent, involved in quality control and affect individual cells or clusters of cells, programmed necrosis has been reported to be a passive process affecting only large fields of cells. Interestingly, necrosis is not initiated due to the activation of one signaling pathway, but as a result of a crosstalk between several signaling pathways (Sun & Peng 2009).

Even though the three PCD assist in the maintenance of tissue regulation and homeostasis, dysregulation of PCD could lead to various diseases, including cancer. It has been reported that the type of PCD activated depends on the nature of the stimulus, time of exposure to the stimulus and the cell environment, because of the extensive cross-talk between the different cell death pathways. Moreover, during cancer development, deficient cell death and tumor resistance to chemotherapy or radiation therapy often occurs; strongly suggesting that PCD might be involved in anticancer therapy. Therefore, targeting PCD pathways may enhance anticancer therapies (Mashima & Tsuruo 2005).

The various programmed cell death pathways namely apoptosis, autophagy and necrosis can be distinguished by their phenotypic characteristics, which affect various organelles, membranes as well as the nucleus of cells (Boujrad et al. 2007). The morphology of cells undergoing apoptosis includes nuclear fragmentation, cell shrinkage, blebbing and membrane bound bodies (Nishida et al. 2008). Autophagy involves the formation of the autophagosome leading to double-membrane bound vesicle structures surrounding the cytoplasmic contents. The double-membrane vesicle fuses with the lysosome resulting in the degradation of the cytoplasmic contents (Chen et al. 2010; Li et al. 2011; Liu et al. 2011). Cell swelling, appearance of empty space in the cytoplasm, disruption of plasma membrane and preservation of the nucleus is associated with programmed necrosis (McCall 2010; Wu et al. 2012). Considering the information presented later in this

report, PCD I (apoptosis) and PCD II (autophagy) will be discussed in more detail.

1.3.1 Apoptosis

Tremendous advances regarding the genetics and biology of cancer has gained interest, and one of the best achievements is the characterization of PCD I. It is extensively reported that mutations of certain oncogenic genes resulting in apoptosis suppression lead to tumor initiation, progression and metastasis (Liu et al. 2011). Thus, more effective research needs to be done in order to uncover the various molecular mechanisms underlying apoptosis in the hope of improving anticancer therapies.

Kerr et al first described apoptosis in 1972, and since then it has received great attention (Ouyang et al. 2012). Apoptosis plays an important role in maintaining cell populations and acts to protect against toxic compounds. It can be triggered by intracellular signals in response to cellular stress such as: oxidative damage caused by reactive oxygen species (ROS), chemotherapeutic drugs, increased calcium concentration and hypoxia (Annunziato et al. 2003; Shimizu et al. 1996). Extracellular signals can also trigger apoptosis by bacterial pathogens, nitric oxide, toxins, hormones as well as growth factors (Brüne 2003; Su et al. 2013).

Intrinsic pathway

The intrinsic or mitochondrial apoptotic pathway is triggered when cells sense intracellular signals such as DNA damage or nuclear instability. These stimuli then activate pro and anti- apoptotic family members consequently leading to the permeabilization of the mitochondria.

The Bcl-2 family members include the anti-apoptotic family (Bcl-2, Bcl-xL, Bcl-w and Mcl-1), which are involved in protecting cells from cytotoxic agents. The pro-apoptotic family includes promoters containing various BH domains and BH3-only members with a single BH domain. The promoters Bax, Bak and Bok are often found on the outer membrane of the mitochondria and regulate apoptosis in a positive manner. The BH3-only members are divided into sensitizers and direct activators. The sensitizer members Bad, Noxa, Bik, Hrk, and PUMA bind and inhibit anti-apoptotic Bcl-2 members whereas the activators Bid and Bim interact with Bax, Bak and Bok. Moreover, Bid and Bim can stimulate Bax and Bak homodimerization leading to the disruption of the outer mitochondrial membrane (figure 1.2).

The mitochondrial outer membrane permeabilization (MOMP) induces cytochrome c release into the cytosol. Cytochrome c recruits Apaf-1 (Apoptotic protease activating factor 1) and pro-caspase 9 in the presence of ATP. Cytochrome c, Apaf-1 and procaspase 9 then form a complex called the apoptosome. Both pro-caspase and caspase 9 contains the protein interaction domain CARD (caspase activation and recruitment domain). This domain facilitates the binding and activation of pro-caspase and caspase 9 with Apaf-1. Once activated, caspase 9 then activates and cleaves pro-caspase 3 to its active form caspase 3, which is an executioner of apoptosis.

Other important proteins such as Smac/Diablo (second mitochondria-derived activator of caspases/Direct IAP-binding proteins with low pI), HtrA2/Omi (High temperature requirement/Omi stress regulated endoprotease) and AIF (Apoptosis inducing factor) are also released from the mitochondria. Smac/Diablo and HtrA2 proteins act by blocking the IAP (Inhibitor of apoptosis protein) family, which comprise eight endogenous caspase inhibitors that prevent apoptosis from occurring (Fulda & Debatin 2013). The IAP family includes various proteins such as XIAP (X-linked inhibitor of apoptosis), cell IAP1 (cIPA1) and cell IAP2 (cIAP2), survivin, neuronal apoptosis inhibitory protein (NAIP), Bruce (Apollon) and ILP-2. Among this family, XIAP has been reported to be the strongest anti-apoptotic protein. It

blocks apoptosis by inhibiting caspase 9 activation and by binding to caspases 3 and 7 (Fulda & Pervaiz 2010).

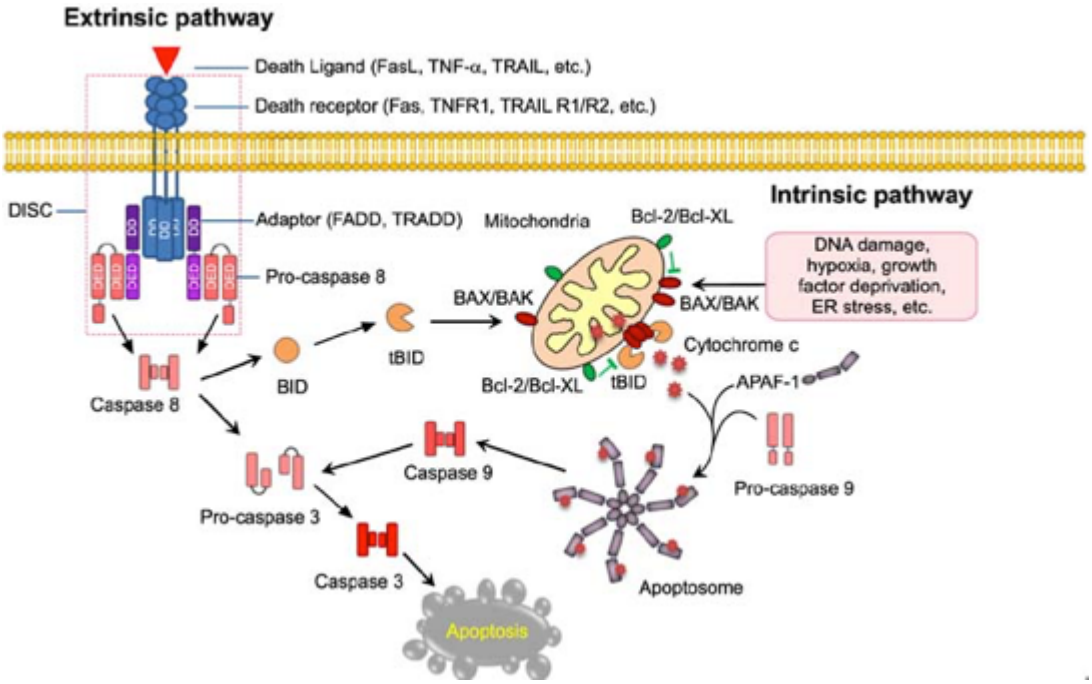

Figure 1.2: The apoptotic pathways. The binding of FasL, TNFα and TRAIL to Fas, TNFR1 and TRAIL R1/R2 activates the extrinsic pathway and this allows the recruitment of FADD or TRADD. The latter recruits caspase 8 and activates caspase 3. Pro-apoptotic Bcl-2 and Bcl-xL and anti-apoptotic Bax and Bak mediate the intrinsic pathway. Stimuli such as DNA damage, hypoxia and ER stress cause PUMA and Bim to inhibit Bcl-2 and Bcl-xL. This allows permeabilization of the outer mitochondrial membrane by Bax/Bak, which consequently results in the release of cytochrome c. Released cytochrome c in turn activates, both caspases 9 and 3 (Sarvothaman et al. 2015).

Extrinsic pathway

The extrinsic or death receptors (DR) pathways play an important role in apoptosis. DRs belong to the tumor necrosis factor (TNF) receptor family, which comprises various proteins. These proteins function by regulating cell death and survival as well as differentiation and immune system regulation (Debatin & Krammer 2004). To date, eight members have been reported and these include tumor necrosis factor receptor 1 (TNFR1), Fas (fatty acid synthetase) or CD95, DR3, TNF-related apoptosis-inducing ligand receptor 1 (TRAILR1), TRAILR2, DR6, ectodysplasin A receptor (EDAR) and nerve growth factor receptor (French & Tschopp 2003).

The extrinsic pathway relies on the Fas death receptor which is activated by Fas-L (Fas ligand) / Fas model (Zapata et al. 2001). Upon ligand binding, Fas-L combines with Fas resulting in a Fas-Fas-L death complex. This complex then interacts with FADD (death domain-containing protein) and procaspase 8 (initiator caspase) forming a death inducible signaling complex or DISC (Lavrik et al. 2005). The activation of DISC results in caspase 8 cleavage, which in turn activates procaspase 3 and Bid. The truncated Bid translocates into the mitochondria to activate Bax/Bak, causing the permeabilization of the mitochondrial outer membrane and release of cytochrome c, which in turn activates caspase 3 (Liu et al. 2011) (figure 1.2).

1.3.2 Autophagy

1.3.2.1 Function of autophagy in cancer cells

Autophagy, a term referring to ‘’ eat oneself ‘’ (auto (self) and phagy (to eat)) is activated by various stimuli including radiation, treatment with various chemical compounds (Bufalin, Ursolic acid), nutrient starvation, accumulation of misfolded proteins in the endoplasmic reticulum, hypoxia and oxidative

stress (Chen et al. 2010; Yang & Klionsky 2010; Shen, Zhang, Wang, et al. 2014b).

Typically, macroautophagy, microautophagy and chaperone-mediated autophagy (CMA) are the three forms of autophagy that have been recognized so far (Mizushima & Komatsu 2011). Macroautophagy or autophagy plays a role in the fusion of the complete autophagosome structure with the lysosome. Microautophagy, however, is poorly described but is thought to be a non-selective form of degradation involving the engulfment of the cytoplasm by the lysosomal membranes. CMA involves targeting and transferring cytosolic proteins into the lysosome for degradation (Das 2015). Targeted proteins must have a specific amino acid sequence that is recognized by HSPA8/HSC70. Once recognized, the cargo is then directed for degradation (Gottlieb et al. 2015).

Autophagy is a catabolic process involved in normal development, senescence, invasion, defense and in various pathological conditions including cancer (Klionsky & Emr 2000; Levine & Klionsky 2004; Meijer & Codogno 2004). One of the main functions of autophagy is to maintain cell survival during stress. Autophagy also plays a role in protein and organelle quality control to avoid the accumulation of unfolded proteins (Komatsu et al. 2005; Wang & Klionsky 2003). Autophagy was also reported to play a role in conditions of stress. For example, DNA damage caused by chemotherapeutic agents, hypoxia or irradiation therapy results in the activation of autophagy, which consequently leads to autophagy cell death (Chen & Karantza-Wadsworth 2009; Klionsky & Emr 2000; Mathew et al. 2007; Papandreou et al. 2008).

Autophagy was primarily considered a pro-survival mechanism, to allow cells to acquire sufficient nutrients under unfavorable conditions. However, there is evidence in the literature suggesting that autophagy can also result in cell death under certain conditions (Liu & Levine 2015). A study conducted by Shimizu et al, 2004, showed that by treating Bax/Bak double-knockout

mouse embryonic fibroblast with etoposide or staurospine, the mouse died in a non-apoptotic way with an increase in vacuoles observed (Shimizu et al. 2004). In the same study, it was shown that the non-apoptotic death of mouse fibroblasts was suppressed by 3-methyl adenine (3-MA) an inhibitor of autophagy), concluding that this mechanism of cell death occurred through autophagy (Shimizu et al. 2004). In addition, Chen et al., 2008 demonstrated that hydrogen peroxide (H_2O_2) and 2-methoxyestradiol (2-ME) caused autophagic cell death in the transformed cell line HEK293 as well as Hela and U87 cell lines. Moreover, it was shown in this study that blocking the accumulation of autophagasome through 3-MA or knocking down autophagy genes Beclin1, ATG5 and ATG7, inhibits oxidative stress induced-cell death. Furthermore, blocking ROS generation also inhibited autophagy induced-cell death (Chen et al. 2008).

Autophagy has developed as an area of interest over the past years as a result of the discovery of AuTophaGy-related (*Atg*) family genes. These genes were first investigated in yeast but their mammalian orthologues have been identified (Inguscio et al. 2012). For the sake of this study, mammalian orthologues will be discussed. Currently, 31 Atg proteins have been identified that participate in the molecular regulation of autophagy and most of them participate in the formation of the autophagosome structures, central to the autophagy process (Suzuki et al. 2007).

1.3.2.2 The Autophagy pathway

The autophagy process involves three main stages: initiation of the pre-autophagosome, elongation of the autophagosome and maturation of the autophagosome. The initiation of the pre-autophagosomal structure involve interactions between various proteins resulting in an enclosed double-membrane structure (or autophagosome) that fuses with lysosomes forming autolysosomes responsible for degrading its content (He & Klionsky 2009). Four different complexes are involved in the initiation process: two kinase

complexes (mTOR C1 and ULK1/2) (figure 1.3) and two ubiquitin-like conjugation systems (Inguscio et al. 2012).

The first kinase complex consists of the mammalian Target of Rapamycin (mTOR), which regulates the autophagy process (He & Klionsky 2009) (figure 1.3). Under nutrient-rich conditions, mTOR inhibits autophagy by phosphorylation of the ULK1/2 complex (unc-51-like kinase: mammalian homologs of Atg1). In nutrient-poor conditions, mTOR dissociates from the ULK1/2 complex, which dephosphorylates ULK1/2. This then causes dephosphorylation and activation of Atg13 and Atg17 (or focal adhesion kinase family-interacting protein of 200 kDa, FIP200). The autophagy initiation is completed when the ULK1/2-ATG13-FIP200 complex accumulates at the site of the phagophore (He & Klionsky 2009; Ohsumi 2000).

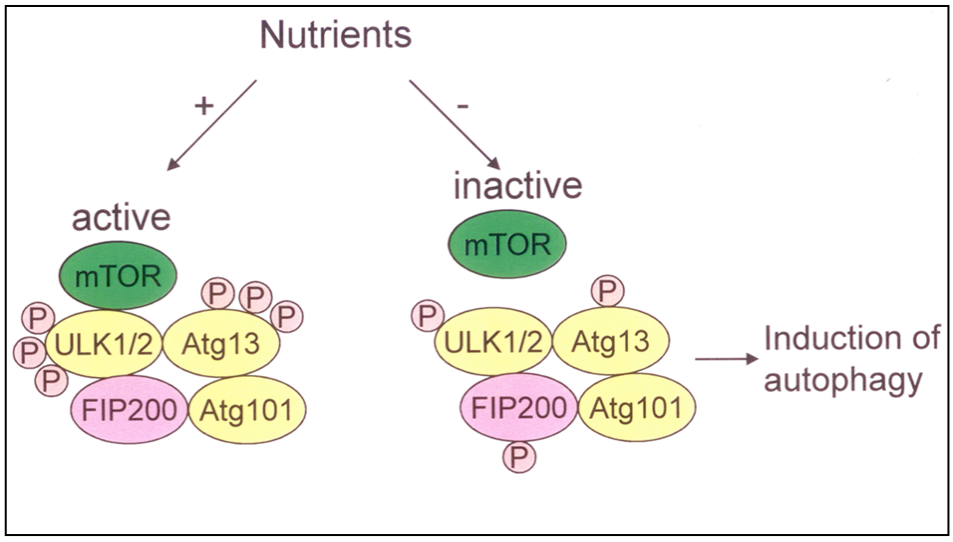

Figure 1.3: mTOR regulates the autophagy process in nutrient-rich and nutrient-poor conditions. In nutrient-rich conditions, active mTOR associates with and hyperphosphorylates ULK1/2, this in turn results in the hyperphosphorylation of Atg13 and therefore subsequently inhibiting autophagy. In nutrient-poor conditions, mTOR dissociates from ULK1/2, causing hypophosphorylation of ULK1/2 complex, Atg13 and phosphorylation of FIP200, thus activating autophagy (Zeng & Kinsella 2011).

In mammalian cells, class I, II and III PI3K have been identified, with class I and III involved in the regulation of autophagy. Class I members cause the inhibition of autophagy. However, the class III, the hVPS34 (human Vesicular protein sorting 34) (figure 1.4) and its subunits including p150 (hVPS15 or phosphoinositol-3-kinase regulatory subunit 4), Beclin1 (Atg6 or Vps 30, a coiled-coil, myosin-like Bcl-2 interacting protein) and Atg14L are necessary for the induction of autophagy and initiation of the pre-autophagosome structure (Jackson & Seaman 1999; Sun et al. 2008) (figure 1.4).

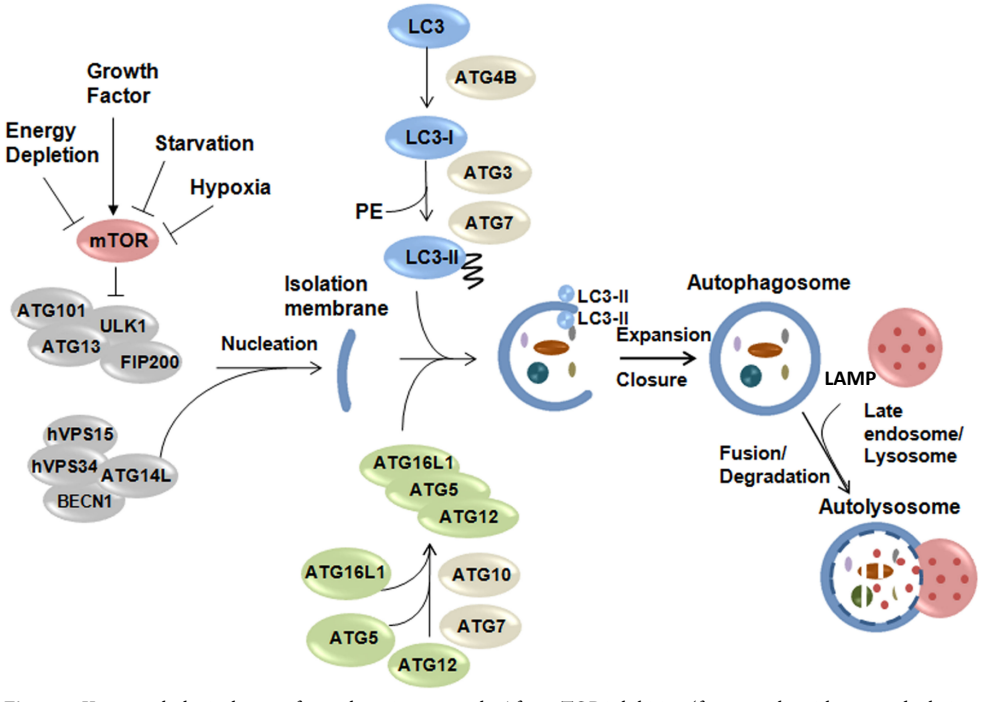

Figure 1.4 Autophagy pathways: During autophagy initiation, the class III PI3K including hVPS34-Beclin1 complex are necessary for recruiting Atg12-Atg5-Atg16L1 and LC3-PE complexes. These complexes function together to elongate the phagophore resulting in the complete autophagosome structure or mature autophagosome. The fusion of the autophagosome with the lysosome/endosome results in autolysosome. Autolysosome contains hydrolytic enzymes, which are responsible for degrading materials in the autophagosome (Karakaş & Gözüaçik 2014).

As mentioned earlier, the class III PI3K members are necessary for the formation of the autophagosome, in which two conjugation systems are necessary (figure 1.4). The first system includes Atg5, Atg12 and Atg16L1. The linkage of Atg12 and Atg5 proteins is mediated by Atg7 (an E1 activating enzyme) and Atg10 (an E2 conjugating enzyme) (Geng & Klionsky 2008). The Atg12-Atg5 complex, interacts with Atg16L1 to form Atg12-Atg5-Atg16L1 complex (Ohsumi & Mizushima 2004) (figure 1.3). This complex localizes to the phagophore, thereby enabling the elongation process (Suzuki et al. 2007) (figure 1.4).

The second system involved in the expansion of the pre-autophagosome structure is LC3-PE (phosphatidylethanolamine) (Suzuki et al. 2001; Suzuki et al. 2007). The precursor protein LC3 is cleaved by the cysteine-protease Atg4B thus generating LC3-I. LC3-I is then activated by Atg7 and transferred to Atg3, a conjugating enzyme (Nakatogawa et al. 2012). The Atg12-Atg5-Atg16L1 complex facilitates the LC3-PE complex by conjugating LC3-I to PE thus generating LC3-II (Mizushima et al. 1999; Mizushima et al. 2003). LC3-II is frequently used to monitor the process of autophagy due to its localization on the outer and inner autophagosome membrane and association with the autophagosome (figure 1.4).

The autophagosome undergoes a first process regulated by the small GTPase Rab7 before fusion with the lysosome (Gutierrez et al. 2004). The second and final process involves fusing the autophagosome with the lysosome/endosome and this process is mediated by LAMP (lysosome – associated membrane protein) (figure 1.4). Fusion of the autophagosome to the lysosome results in autolysosome wherein hydrolytic enzymes such as cathepsins B, D and L degrade sequestered material (He & Klionsky 2009). The amino acids and lipids generated by the lysosomes can be used as an energy source and building blocks especially in starvation conditions (Inguscio et al. 2012).

1.3.2.3 The role of autophagy in cancer

Autophagy seemingly has dual roles in cancer because of its role in cell survival and cell death processes (White & DiPaola 2009). Depending on the stage of cancer, autophagy can be a tumour suppressor mechanism at the early stage of cancer or promote tumourigenesis (Brech et al. 2009).

Autophagy can act as a tumour suppressor mechanism based on its frequent down-regulation in tumours (Inguscio et al. 2012). Beclin1 has been extensively reported as a tumour suppressor due to the allelic deletion of the gene encoding Beclin1 *BECN1* in human ovarian, breast and prostate cancer (Shimizu et al. 2004). Moreover, many studies have demonstrated that mice with Beclin1 mutations were prone to tumours, suggesting the tumour-suppressing role of Beclin1 (Qu et al. 2003; Yue et al. 2003). Beclin1 can also interact with endophilin B1 (Bif-1) and act as a tumour suppressor. The interaction of Beclin1 with Bif-1 via UVRAG activates Vps34 resulting in the formation of autophagosome. Loss of Bif-1 is often associated with a wide variety of human cancer such as gastric carcinoma, colorectal carcinoma and urinary cancer (Ionov et al. 2004; Takahashi et al. 2005).

Autophagy has also been implicated in cell survival processes in various cancer cells (Inguscio et al. 2012). Due to its role in supplying nutrients from cytoplasmic breakdown, autophagy can enable metastasized cancer cells to tolerate stressful conditions, hypoxia, nutrient deprivation and the effect of anti-cancer drugs such as cisplatin and camptothecin (Lock & Debnath 2008). Interestingly, knockdown or genetic inhibition of important autophagy role-players such as Atg5 or beclin1 in cancer has been shown to induce autophagy cell death (White & DiPaola 2009).

Understanding the function of autophagy in tumourigenesis is crucial since some anticancer drugs and pharmacological agents have been reported to induce autophagy (Shen, 2014; Wong et al. 2013). Moreover, autophagy can

either promote survival or death in cancer cells as discussed above. It seems that the specific role of autophagy (cell death or cell survival) in cancer depends on treatment, tissue and is specific to the type of cell line. In addition, several pathways have been involved in the activation of autophagy. Some of those pathways will be discussed in the next section.

1.3.2.4 The regulation of autophagy

Multiple signaling pathways regulate autophagy, presumably reflecting the critical nature of autophagy in cell survival, in conditions of crisis, and in mediating cell death. These signaling pathways include: (1) PI3K/AKT/mTOR (2) AMPK/TSC/mTOR and (3) ER stress/Ca^{2+}/CAMMK/AMPK/mTOR.

The mTOR pathway includes two complexes: mTORC1 and mTORC2. mTORC1 complex has been reported to be involved in autophagy and consists of mTOR, PRAS40 (proline rich AKT substrate of 40kDa), RAPTOR (regulatory associated protein of mTOR) and mLST8 (mammalian lethal with sec-thirteen protein 8, also known as GβL) (Gwinn et al. 2008; Inoki et al. 2003; Wullschleger et al. 2006). The PI3K-AKT-mTOR pathway constitutes the inhibitory pathway controlling autophagy and is activated by the binding of the insulin-like growth factor (IGF) to the insulin receptor (IR) resulting in the activation of PI3K (figure 1.5). Activated PI3K converts phosphatidylinositol-3,4-bisphosphate, phosphatidylinositol-4,5 bisphosphate (PIP_2) to phosphatidylinositol-3,4,5 trisphosphate (PIP_3). This then causes phosphoinositide-dependent kinase (PDK1) and AKT to the recruited at the cell membrane. Phosphorylated and activated AKT results in the inhibition of the TSC1/2 complex (Tuberous sclerosis factor 1 and 2) by phosphorylation of TSC2 (Alessi et al. 1997; Stokoe et al. 1997). Inhibited TSC1/2 complex activates the small GTPase Rheb (Ras Homolog Enriched in Brain), which in turn is able to activate mTOR, resulting in the inhibition of autophagy. PTEN (Phosphotase and tensin homolog deleted on chromosome 10) stimulates

autophagy by inhibiting the PI3K/AKT pathway (Arico et al. 2001) (figure 1.5).

Metabolic and energy stress induces autophagy through the activation of the AMPK-mTOR pathway in mammalian cells. In these cells, AMPK (AMP-activated protein kinase) phosphorylates and activates the TSC1/2 complex, allowing the phosphorylation of TSC2 by GSK-3β (glycogen synthase kinase 3). Phosphorylation of TSC2 results in the inhibition of the mTOR through the small GTPase Rheb (figure1.5) (Inoki et al. 2003; Shang & Wang 2011).

ER stress is also responsible for calcium release from the ER into the cytoplasm, which results in the phosphorylation and activation of calcium-activated calmodulin-dependent kinase kinase-β (CaMKKβ), leading to the activation of AMPK and autophagy (Høyer-Hansen et al. 2007) (figure 1.5).

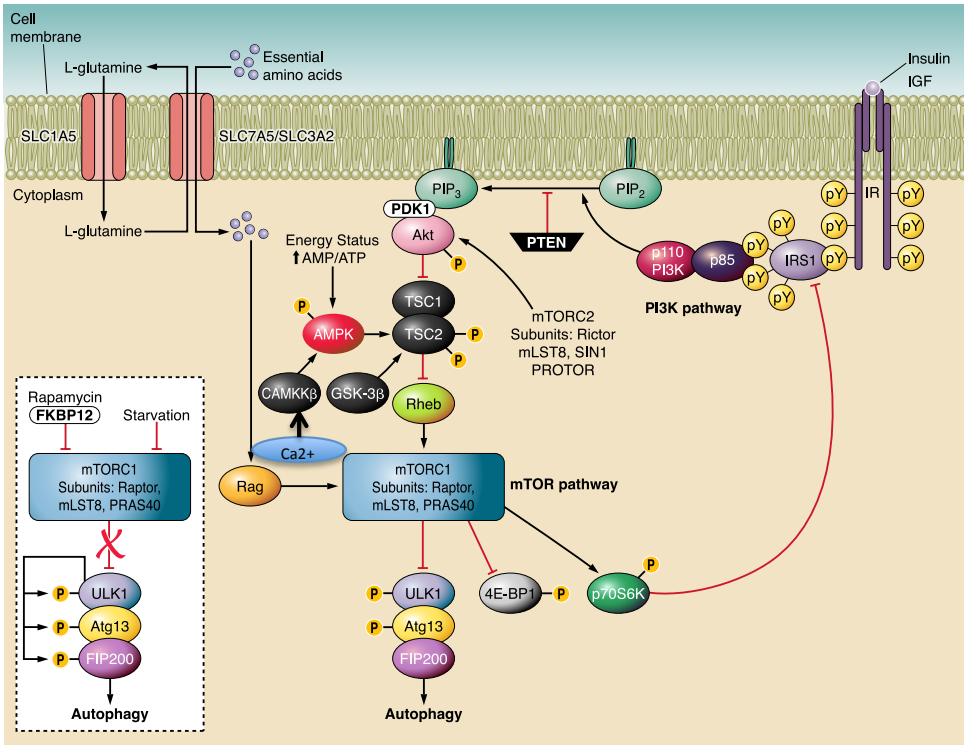

Figure 1.5: Pathways involved in the regulating of autophagy. The PI3K-AKT-mTOR pathway blocks the autophagy process. AMPK activates autophagy by phosphorylating and activating the TSC1/2 complex. This complex inhibits the mTOR pathway and can also be activated by calcium (CAMKKβ) (Adapted from Ravikumar et al. 2010).

Numerous studies support the idea that autophagy is induced by ER stress in mammalian cells (Yorimitsu et al. 2006; Younce & Kolattukudy 2010). ER stress can be induced by various factors that include treatment with accumulation of misfolded proteins, hypoxia, a decrease in glucose and chemotherapeutic agents (Høyer-Hansen & Jäättelä 2007). Once the ER stress occurs, the unfolded protein response (UPR) is induced to alleviate the stress by either inhibition of protein synthesis or upregulation of protein folding and degradation pathways. Three pathways regulate the UPR: the activating transcription factor 6 (ATF6), inositol requiring enzyme 1 (IRE1) and PRK (RNA-dependent protein kinase) - like ER kinase (PERK) (Ogata et al., 2006 (figure 1.6). Studies showed that treatment of mouse embryonic fibroblasts (MEFs) and cancer cells with tunicamycin activated the

phosphorylation of c-Jun N-terminal (a downstream target of the IRE1 pathway), which then leads to autophagy (Ding et al. 2007; Ogata et al. 2006). Other studies conducted on murine cells reported that the expression of misfolded polyQ72 or mutant dyferlin proteins induced ER stress, leading to the phosphorylation of eIF2α (a downstream target of PERK). This resulted in the conversion of LC3 and the degradation of the mutant proteins within the ER organelle (Fujita et al. 2007). These studies concluded that the IRE1 and PERK pathways play important roles in UPR-induced autophagy.

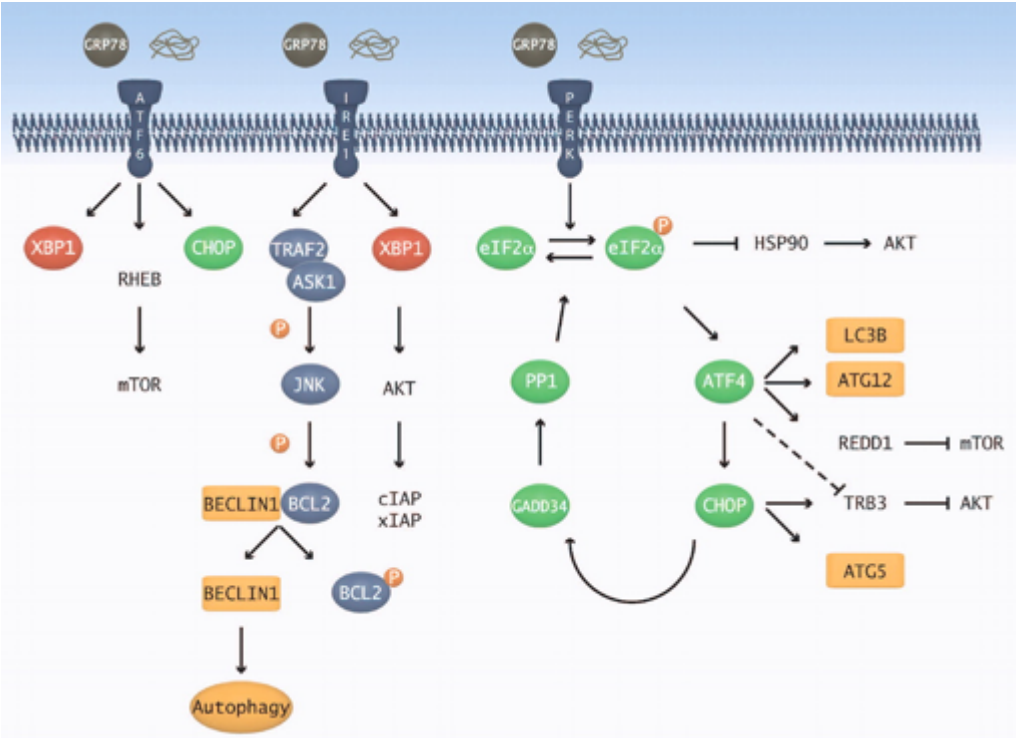

Figure 1.6 Relationship between the ER stress pathways and autophagy. The three ER stress sensors are held inactive by the GRP78 proteins. When the unfolded proteins accumulate, the GRP78 dissociates from the sensors, resulting in their activation. The PERK and IRE1 have been implicated in autophagy. In the IRE1 branch, BCL2 is phosphorylated by JNK, which result in the release of BCL2 from Beclin1, thus activating autophagy. In the PERK branch, ATF4 and CHOP cause the upregulation of LC3B, ATG12 and ATG5 (Aronson & Davies 2012).

Studies have implicated ROS as an intracellular stressor that induces autophagy. It has been reported that excessive ROS generation upon treatment with anticancer agents leads to autophagic cell death (Yu et al. 2006).

Section 1.3 described the PCD that cancer utilizes to maintain cell homeostasis, development as well as survival. When these PCDs are disrupted, cancer occurs. Cells contain a variety of death pathways; an understanding and manipulation of these pathways by anticancer agents may help in fighting the disease

A diverse range of anticancer drugs are currently utilized for the treatment of various cancers. However, these chemotherapeutic agents are often associated with unwanted toxicity. Therefore, there is a need to develop novel anticancer compounds that can specifically targeted cancer cells while sparing normal cell. Novel anticancer agents employed to target cells elicit their effect by manipulating the PCD's previously described. Generally the preferred PCD chosen by researchers is PCD II or apoptosis, although this causes a limitation in the understanding of other PCD such as autophagy. Cancer cells are often resistant to chemotherapeutic treatment, and therefore exploiting or developing compounds that can target and activate more that one programmed cell death will help in improving cancer treatment. Until now, the main interest in cancer research has been to improve therapies by determining either the effect of newly discovered anticancer drugs or various drugs effective against other diseases. The artemisinins represent a family of compounds with great potential that can be used as source for novel anticancer compounds. Moreover, a possible role of artemisinin derivatives in overcoming drug-resistant cases has also been reported (Enzinger & Mayer 2003; Gottesman 2009)

On the basis of these remarkable features, dihydroartemisinin the most potent artemisinin compound was covalently conjugated to isatin an indole derivative by the chemistry department of the University of Cape Town. The final product was a novel isatin-artemisinin derivative named EXP57EA. In this study we explored the activity of this novel compound to kill cancer cells and to understand the mechanism of cell death as a follow on of earlier studies performed in our laboratory.

1.4 Project Aim and Objectives

Determine the effect of EXP57EA on a panel of cancer cell lines by,

(1) Comparing the cytotoxicity effect of EXP57EA, DHA and Cisplatin

(2) Determining the mode of cell death caused by EXP57EA on a panel of selected cancer cell lines and

(3) Investigating the signaling pathways triggered by EXP57EA in WHCO1 and WHCO5 cell lines.

CHAPTER 2:

RESULTS

2.1 Determine the cytotoxicity of artemisinin derivatives

Artemisinins and its derivatives have been widely used in the treatment of malaria for several years (Maria P Crespo-Ortiz & Wei 2012), and recently this family of compounds was shown to have antiviral and antimicrobial activities as well as strong anticancer activity *in vivo* and *in vitro*. A study conducted by Xu et al., in 2011 demonstrated that the artemisinin derivative artesunate may be used as a chemotherapeutic agent in highly metastatic and aggressive cancers *in vitro and in vivo* (Xu et al. 2011). Colleagues from the Chemistry Department at the University of Cape Town designed a novel hybrid compound, by covalently conjugating the most potent artemisinin compound Dihydroartemisinin (DHA) with an iodo-isatin azide intermediate compound using click chemistry and a novel hybrid compound was generated, namely EXP57EA (figure 2.1). The strategy behind the design of compound EXP57EA is discussed in a previous thesis (Shunmoogam-Gounden 2014).

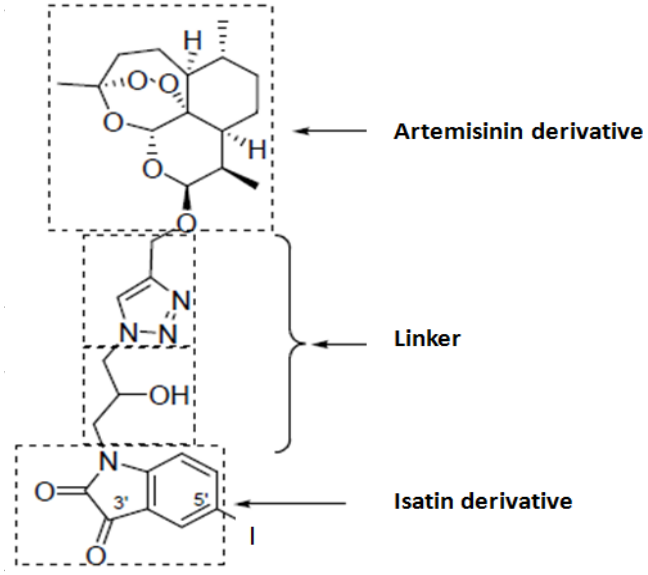

Figure 2.1: Structure of EXP57EA. Structures showing the two compounds that were covalently conjugated to form the novel artemisinin-isatin hybrid compound.

The results presented in this section examined the cytotoxic effect of the novel hybrid compound EXP57EA compared to the parental compound DHA, which has been reported to be the most potent artemisinin-like compound (Maria P. Crespo-Ortiz & Wei 2012). Moreover, the cytotoxic effect of cisplatin, a drug commonly used as single or combination therapy in the treatment of various cancers was also compared to that of the novel hybrid compound.

The cytotoxicity of DHA, EXP57EA and cisplatin was determined on a panel of cancer cell lines including three esophageal cancer (OC) cell lines WHCO1, WHCO5 and KYSE150 which are routinely used as model esophageal cancer cell lines in our laboratory (Hadley & Hendricks 2014; Van Der Watt et al. 2014), one metastatic breast cancer cell line MDA-MB-231 and one cervical cancer cell line SiHa. For the cytotoxicity assay, cell number was estimated using the MTT (3 [4, 5-dimethylthiazol-2-yl] -2, 5-diphenyltetrazolium bromide) assay and GraphPad prism software was used to generate dose response curves and IC_{50} values (concentration of the drug required to kill 50 % of the cells) (figure 2.2).

Screening EXP57EA against the panel of cancer cell lines showed that EXP57EA displayed activity across all cell lines. EXP57EA was more active in WHCO1 915.8 μM) and WHCO5 (20 μM) than in KYSE150 (29.2 μM), MDA-MB-231 (22.1 μM) and SiHa (25.1 μM) (table 2.1). EXP57EA was more active across all cell lines compared to DHA, which in turn was active against two cell lines: the esophageal cancer cell lines: WHCO1 (21.3 μM) and WHCO5 (77.3 μM). DHA displayed no cytotoxicity in KYSE150, MDA-MB-231 and SiHa cell lines in the concentration range tested (0 μM – 200 μM) (table 2.1). It was reported that MDA-MB-231 and SiHa cell lines are resistant to certain chemotherapeutic agents including cisplatin (Yde & Issinger 2006) and this was confirmed in this study where DHA was not active in MDA-MB-231 and SiHa. Here, cisplatin displayed decreased sensitivity to the same cell lines.

Cisplatin was less active in OC cell line WHCO1 with an IC_{50} value of 48.5 μM compared to DHA, with an IC_{50} value of 21.3 μM. However, cisplatin was more active in WHCO5 (31.2 μM), KYSE150 (86 μM), MDA-MB-231 (108.1 μM) and SiHa (71.1 μM) cell lines than DHA (table 2.1). It was also found that the novel hybrid compound EXP57EA was more active than cisplatin across all cell lines (table 2.1).

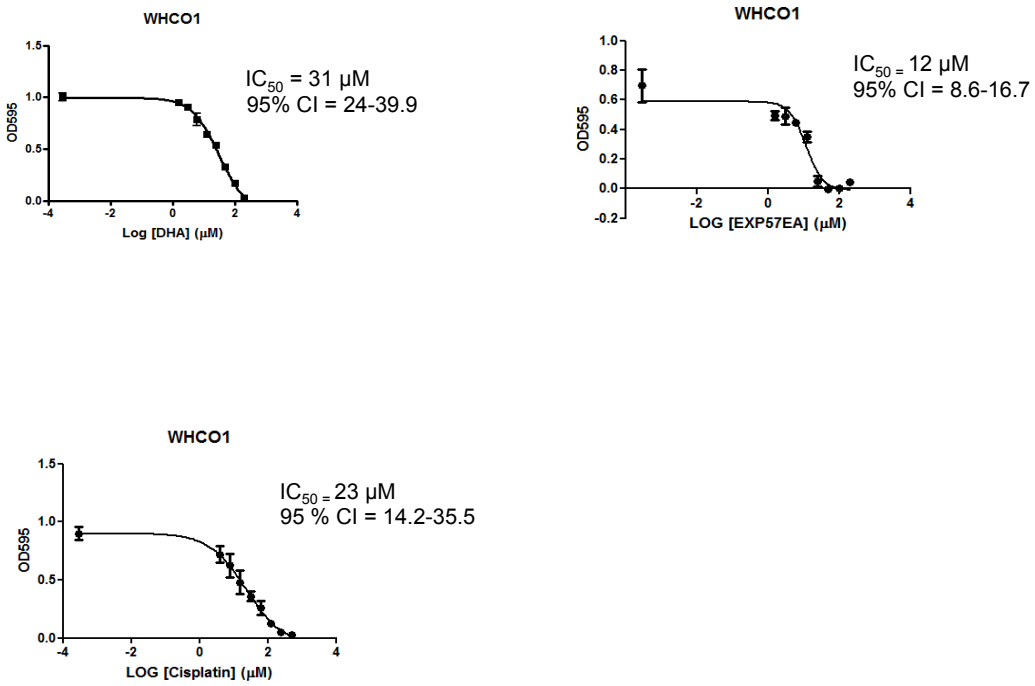

Figure 2.2: IC_{50} curves showing sensitivity of WHCO1 cells to DHA, EXP57EA and cisplatin. Cells were plated at a density of 3000 cells per well in 96 well plates and were treated with a range of concentrations of EXP57EA for 48 hours, followed by MTT assay. The absorbance was read on a plate reader at 595 nm and data were analyzed using GraphPad software. Each point was performed in triplicate and error bars represent the mean ±SD. These figures are representative of three independent experiments.

Table 2.1: IC_{50} values of EXP57A, DHA and cisplatin in a panel of cancer cell lines. The IC_{50} values obtained for EXP57EA, DHA and cisplatin screened against three esophageal cancer cell lines WHCO1, WHCO5 and KYSE150, one breast cancer cell line MDA-MB-231 and one cervical cancer cell line SiHa. The MTT assay was used to measure cell number and GrapPad software was used to calculate the global IC_{50} values and the 95 % confidence interval.

	IC_{50} values (μM) and 95 % Confidence interval (CI)		
	DHA	**Cisplatin**	**EXP57EA**
WHCO1	21.3 (15.4-29.5)	48.5 (36.6-64.3)	15.8 (13.4-18.7)
WHCO5	77.3 (50.7-117.9)	31.2 (27.2-35.8)	19.8 (17.6-22.2)
KYSE150	NA	86 (70.6-104.7)	29.2 (22.6-37.7)
MDA-MB-231	NA	108.1 (77.1-151.4)	22.1 (20.1-24.4)
SiHa	NA	71.1 (58-87.2)	25.1 (22.9-27.6)

*NA = Not active

The purpose of synthesizing novel hybrid compounds is to produce compounds that displayed better activity than their parental compounds (Meunier et al. 2010). The results in this project showed that this has been achieved where EXP57EA displayed greater activity than DHA and cisplatin in all cell lines tested. Hybrid compounds have been reported to be pharmacologically different from their parental compounds by displaying different or better activity from their parental compound (Teiten et al. 2014).
Considering that earlier studies performed in our laboratory suggested that EXP57EA induced autophagy, we investigated the mode of cell death

mediated by EXP57EA, using this compound at 15 μM based on the outcome of the experiments reported in table 2.1.

2.2 The effect of EXP57EA on cultured-cancer cell morphology

Previous studies have shown that DHA induced apoptosis in various cancer cell lines (Hou et al. 2008; Lu et al. 2014). It was shown in our laboratory that esophageal cancer cell lines WHCO1 and WHCO6 treated with 60 μM DHA for 48 hours, displayed the morphological changes indicative of apoptosis. Nuclear condensation and shrinkage of the cytoplasm were observed, later confirmed by PARP cleavage and caspase activity assays (Shunmoogam-Gounden 2014). However, in that study when the same cell lines were treated with EXP57EA, the morphological features were not consistent with apoptosis. Instead after 24 hours and 48 hours treatment, numerous intracellular, perinuclear vacuoles were observed using transmission electron microscopy (TEM) and these changes occurred in a time and dose-dependent manner.

To understand how EXP57EA causes cell death, the cancer cell lines previously mentioned were treated with 15 μM EXP57EA for 24 hours and the morphology of cells were observed using a microscope (figure 2.3). The morphological changes of cells treated with EXP57EA showed various intracellular vacuoles (white arrows). Interestingly WHCO5, KYSE150, MDA-MB-231 and SiHa cells showed signs of autophagy (vacuoles), even though the IC_{50} value of EXP57EA in these cell lines were higher than the WHCO1 cell line. When WHCO1 and WHCO5 cells were treated with 40 μM DHA, cell shrinkage was observed in the treated cells compared to the control, which was indicative of apoptosis. Interestingly, even though KYSE150, MDA-MB-231 and SiHa cells were resistant to DHA, cell shrinkage was seen when the cells were treated with 75 μM DHA, also indicative of apoptosis (figure 2.4).

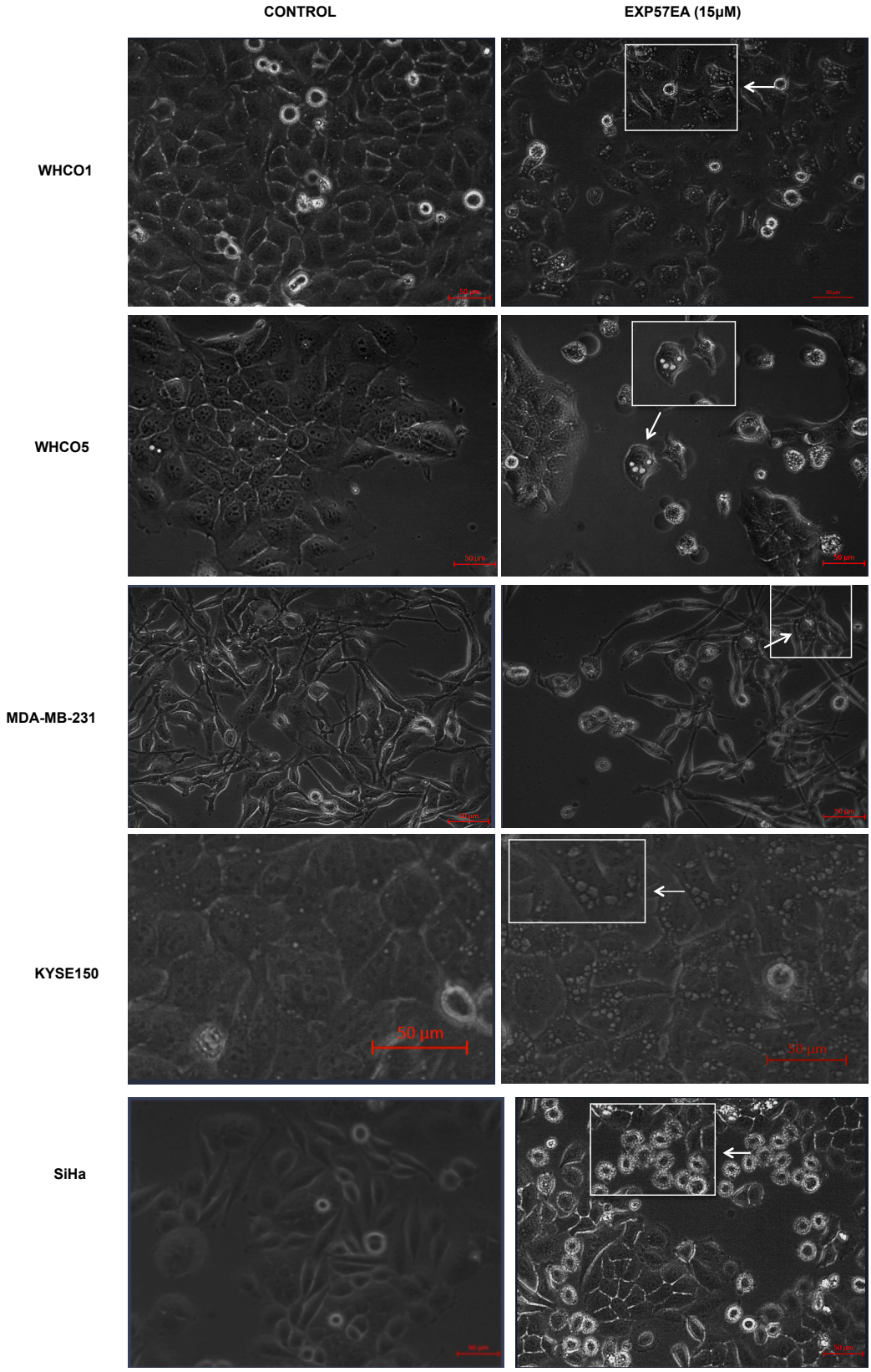

Figure 2.3: The effect of EXP57EA on cell morphology. Cells were plated at a density of 300000 cells per 60 mm dish. (A) Cells were treated with DMSO (control) and (B) 15 μM EXP57EA for 24 hours. After the indicated time, images of the cells

were captured with a Primovert inverted microscopy with an Axio cam ERC 5s (Zeiss, Göttingen, Germany). White arrows point out intracellular vacuoles.

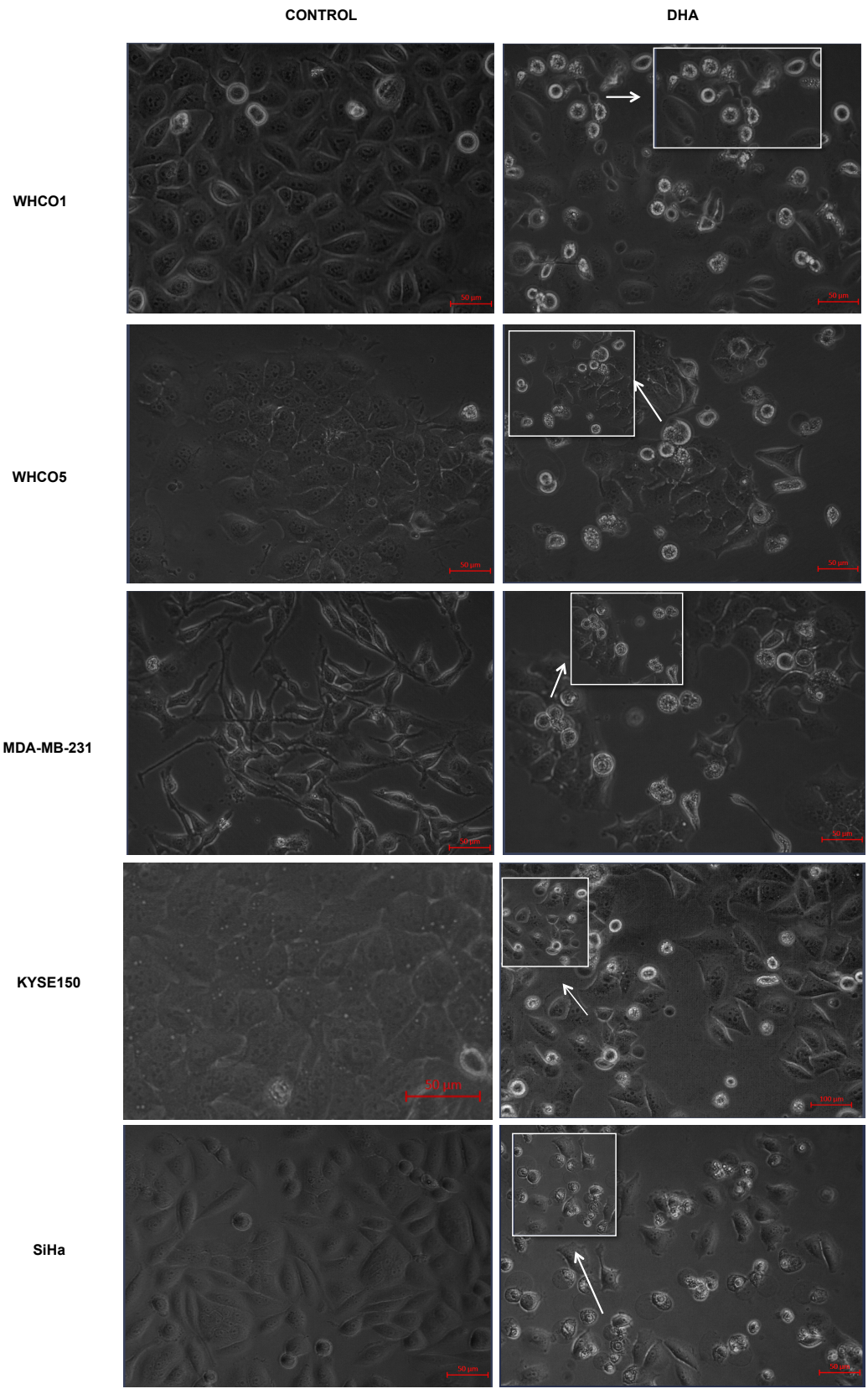

Figure 2.4: The effect of DHA on cell morphology. Cells were plated at a density of 300000 cells per 60 mm dish. (A) Cells were treated with DMSO (control) and (B) WHCO1 and WHCO5 were treated with 40 μM, MDA-MB-231, KYSE150 and SiHa were treated with 75 μM DHA for 24 hours. After the indicated time, images of

the cells were captured with a Primovert inverted microscopy with an Axio cam ERC 5s (Zeiss, Göttingen, Germany). White arrows point out cell shrinkage.

The effect of EXP57EA and its parental compound DHA on cell morphology was examined. The results showed that EXP57EA treatment was associated with the appearance of intracellular vacuoles, suggestive of autophagy. When cells were treated with DHA, cell shrinkage was observed, confirming previous results found in our laboratory.

2.3 Investigate the mode of cell death caused by EXP57EA in the panel of cancer cell lines

The mechanisms by which most anticancer agents cause death is important since there is a general view that apoptosis is the preferred mechanism of cell death in the context of chemotherapeutic treatment of cancer. Moreover, it is the most well characterized mode of cell death (Du et al. 2013).

In order to determine the mode of cell death induced by EXP57EA in the panel of cancer cell lines used here, a PARP (Poly ADP-ribose polymerase) assay was done. PARP is a well-known caspase substrate and its cleavage in two fragments (116 kDa and 85 kDa) is frequently used as a marker of apoptosis (Casao et al. 2015; Chaitanya et al. 2010). PARP cleavage was examined by western blot in WHCO1, WHCO5, KYSE150, MDA-MB-231 and SiHa cells treated with 15 μM EXP57EA for 24 hours. WHCO1 cells were treated with 15 μM Doxorubicin (DOX) and used as a positive control for PARP cleavage. GAPDH was used as a loading control. Cell lines treated with EXP57EA showed no PARP cleavage, however WHCO1 treated with Dox showed PARP cleavage after 24 hours treatment (figure 2.5.A). Furthermore, when the same cell lines were treated with DHA for 24 hours (concentrations mentioned in above section), PARP cleavage was clearly seen in all cell lines (figure 2.5.B). These results showed that EXP57EA did not activate PARP cleavage; instead, its parental compound DHA activated PARP cleavage in all cell lines tested. Moreover, these results confirmed the morphological changes observed in figure 2.3 where no clear signs of apoptosis was seen, instead vacuoles were observed which was suggestive of autophagy.

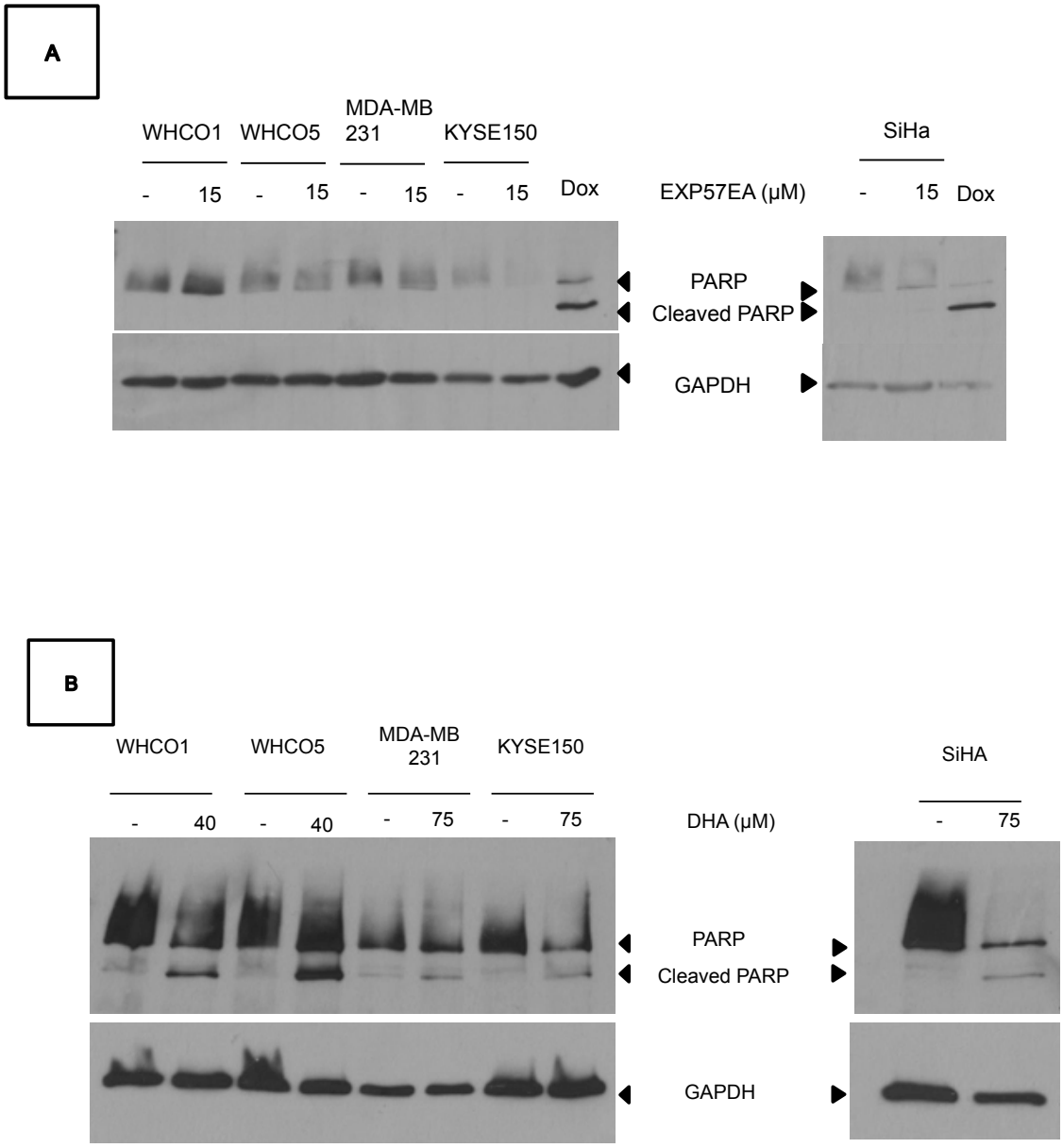

Figure 2.5: Effect of EXP57EA and DHA on PARP cleavage. Cells were plated at a density of 300000 cells per 60 mm dish. (A) The cells were treated with 15 μM EXP57EA and (B) WHCO1 and WHCO5 were treated with 40 μM, MDA-MB-231, KYSE150 and SiHa were treated with 75 μM DHA for 24 hours. Proteins were harvested and 20 μg were separated on a 10 % SDS-PAGE and proteins were transferred to a nitrocellulose membrane. WHCO1 cells were treated with 15 μM DOX for 24 hours and used as a positive control for PARP cleavage (A). GAPDH was used as a loading control. This result is representative of two independent experiments.

We performed further experiments to determine if EXP57EA induced autophagy, since treatment of cells with this compound induced the appearance of vacuoles that resembled autophagic vesicles and failed to induce PARP cleavage (figures 2.3 and 2.5). We used two traditional autophagy markers LC3-II and Beclin1, both involved in autophagy. The aberrant expression of these two markers has been reported in various cancers including melanoma, human colon, ovarian, lung and brain cancer (Aita et al. 1999; Miracco et al. 2007; Yorimitsu & Klionsky 2007). To this end, western blot analysis was performed to examine the expression level of Beclin1, upon EXP57EA treatment. Figure 2.6 showed western blot results of the expression level of Beclin1 after 12 hours and 24 hours treatment. Changes in the expression level of Beclin1 were seen at both 12 hours and 24 hours in all cell lines, however, at 24 hours the expression level of Beclin1 consistently decreased in all cell lines. These results suggested that EXP57EA treatment activates Beclin1.

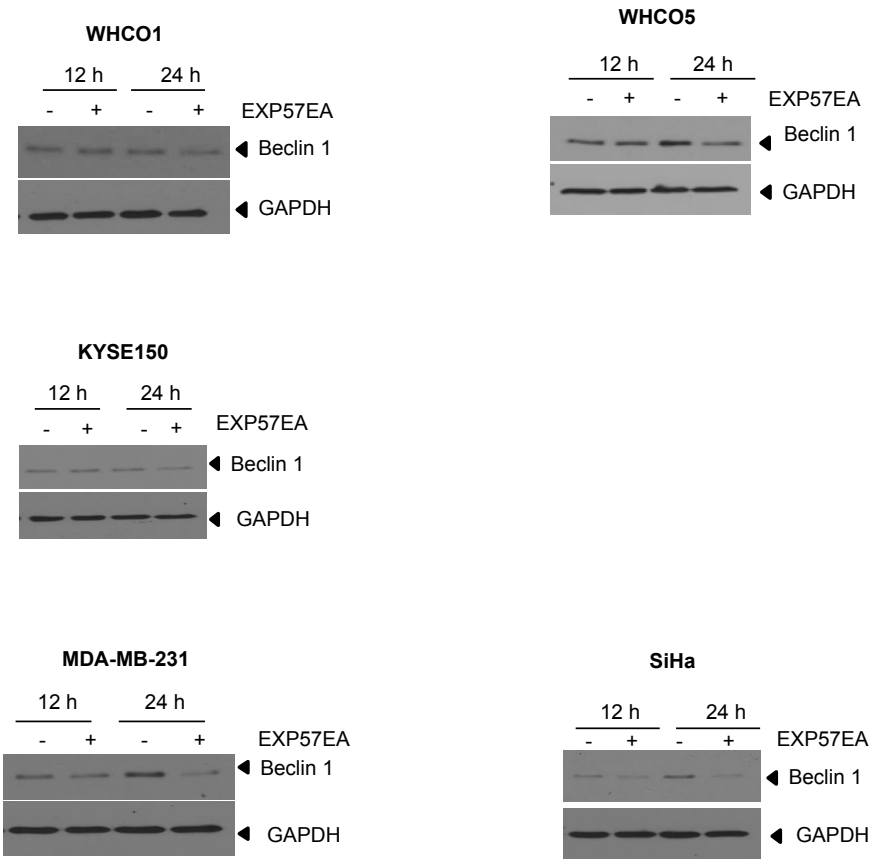

Figure 2.6: Beclin1 expression after treatment with EXP57EA. Cells were plated at a density of 300000 cells per 60 mm dish. The cells were treated with 15 μM EXP57EA for 12 hours and 24 hours. Proteins were harvested and 40 μg were separated on a 10 % SDS-PAGE and proteins were transferred to a nitrocellulose membrane. The membrane was probed with an antibody recognizing Beclin1. GAPDH was used as a loading control and this figure is representative of three independent experiments.

To further confirm that EXP57EA plays a role in the induction of autophagy, the effect of EXP57EA on LC3-II expression levels was also examined by western blot. LC3 protein consists of two forms: the soluble form LC3-I, with a size of 18 kDa and a lipidated form LC3-II, with an apparent size of 16 kDa. Figure 3.7 shows the expression level of LC3-II in the same panel of cancer cell lines, in response to EXP57EA treatment. Treatment with 15 μM EXP57EA caused the activation of LC3-II at 12 hours and 24 hours in WHCO1, WHCO5, KYSE150 and MDA-MB-231 cell lines (figure 2.7).

However, in SiHa treated cells, both at 12 hours and 24 hours, the expression level of LC3-II was low compared to untreated cells. It has been reported that the expression level of LC3-II and Beclin1 protein was significantly decreased in cervical squamous cancer cells than in healthy squamous epithelial cells. This suggests that autophagy may play a tumour-suppressing role in cervical tumourigenesis (Orfanelli et al. 2014).

Our results, which show clear changes in the level of Beclin1 and LC3-II in response to EXP57EA treatment, strongly suggested that this compound induces autophagy. However, these results could also reflect a blockage in the fusion of the autophagosome with the lysosome, resulting in the accumulation of autophagosomes or a deficiency in the lysosomal degradation step, also resulting in the accumulation of autolysosomes (Gukovskaya & Gukovsky 2012; Mizushima & Yoshimori 2007).

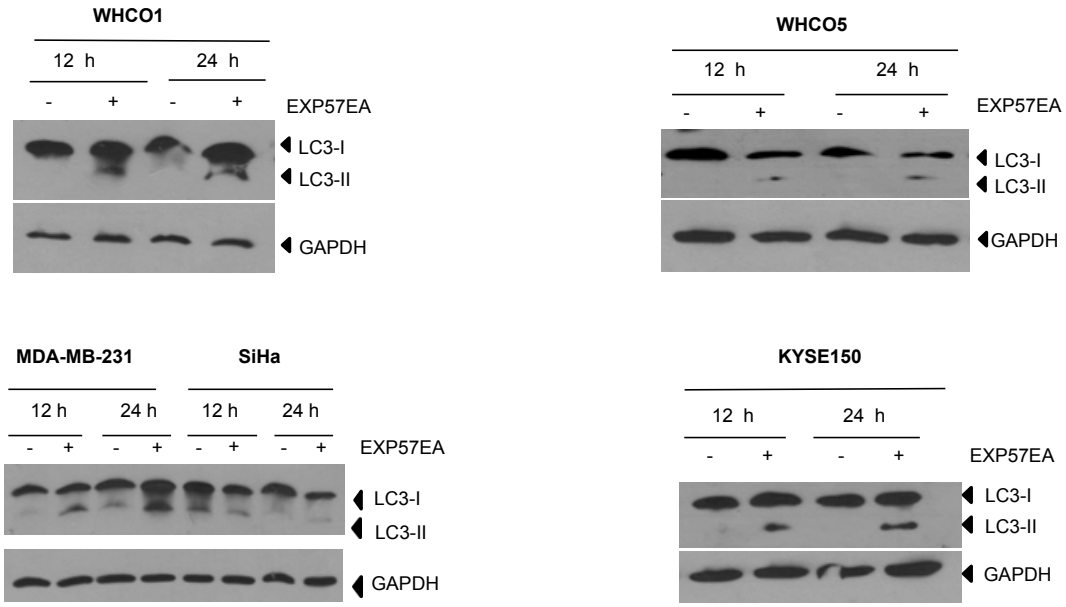

Figure 2.7: LC3-II expression after treatment with EXP57EA. Cells were plated at a density of 300000 cells per 60 mm dish. The cells were treated with 15 μM EXP57EA for 12 hours and 24 hours. Proteins were harvested and 40 μg were separated on a 15 % SDS-PAGE and proteins were transferred to a nitrocellulose membrane. The membrane was probed with an antibody recognizing LC3-I and LC3-II. GAPDH was used as a loading control and this figure is representative of three independent experiments.

In this study, we monitored the activation of autophagy by measuring LC3-II levels in cells. However, autophagy is a multi-step process and changes in Beclin1 and LC3-II levels could be indicative of a blockage in the autophagic process, and not increased autophagic flux. Therefore, the detection of the number of autophagosomes and the assessment of LC3-II by microscopy and immunoblotting respectively are insufficient to conclude if a particular compound activates autophagy (Zhang et al. 2013). There are however, standard methods available to determine whether a particular compound activates autophagy. Among these, is the measurement of autophagic flux by analyzing LC3-II turnover by western blot. This method is based on the observation that LC3-II is degraded in the autolysosome during autophagy (Mizushima et al. 2010).

During the process of autophagy, lysosomal enzymes degrade the cargo within the autophagosome after fusion of the autophagosome with the lysosome to form the autolysosome. Thus, lysosomal enzymes may degrade considerable amounts of endogenous LC3-II on autophagosomes. To investigate lysosomal LC3-II turnover, we employed ammonium chloride (NH_4Cl) and chloroquine. Both compounds block the lysosomal degradation of the autolysosome content by inhibiting the Na^+ /H^+ pump, raising the lysosomal pH and therefore inhibiting acidic lysosomal proteases (Rubinsztein et al. 2009). Cells were pretreated with 10 mM NH_4Cl and 30 uM chloroquine for 1 hour. Figure 2.8 showed that when WHCO1 and SiHa cells were co-treated with EXP57EA and NH_4Cl a significant increase in the expression level of LC3-II was observed compared to cells treated with EXP57EA alone (figure 2.8). When chloroquine was used in WHCO1 cells, the expression level of LC3-II increased significantly in the cells co-treated with EXP57EA and chloroquine compared to cells treated with EXP57EA alone. Klionsky et al. 2016 reported that Increased level of LC3-II in the cells treated with the inhibitor is indicative of autophagic flux carrier to the lysosome (Klionsky et al. 2016) This was confirmed in this study where WHCO1 cells treated with chloroquine alone displayed an increased level of LC3-II. The results showed that EXP57EA increased the synthesis of the autophagosomes and delivery of substrates to the lysosomes. Based on these results we can conclude that EXP57EA increased the autophagic flux in WHCO1 and SiHa cell lines.

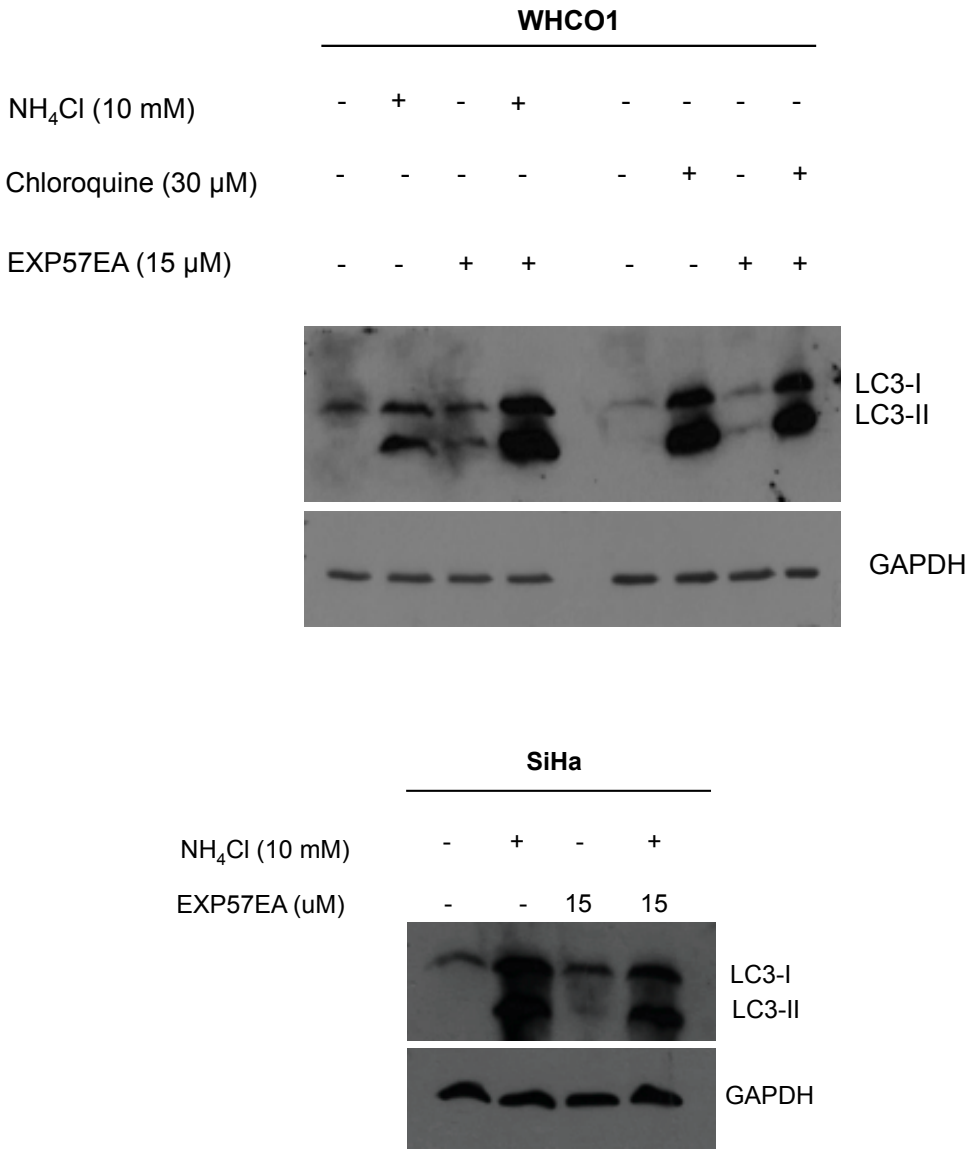

Figure 2.8: The effect of NH_4Cl and chloroquine on LC3-II accumulation. WHCO1 and SiHa Cells were plated at a density of 300000 cells per 60 mm dish. Treatments were as follows: cells were pre-treated for 1 hour with either 10 mM NH_4Cl or 30 μM chloroquine. After 1 hour, the cells were treated with 15 μM EXP57EA for 24 hours. Control cells were treated with DMSO. Proteins were harvested and 40 μg were separated on a 15 % SDS-PAGE and proteins were transferred to a nitrocellulose membrane. The membrane was probed with an antibody recognizing LC3-I and LC3-II. GAPDH was used as a loading control and this figure is representative of two independent experiments.

Having shown that EXP57EA activated autophagy on the basis of (1) changes in the expression level of two important autophagy markers; LC3-II

and Beclin1; (2) increased autophagic flux as well as showing that EXP57EA did not activate PARP, we next investigated the underlying pathways involved in EXP57EA-activated autophagy.

2.4 Investigating the cellular signaling pathway activated by EXP57EA in a panel of cancer cell lines

In the previous two sections, we showed that EXP57EA displayed activity against the cancer cell lines tested and that EXP57EA was more active than DHA and cisplatin when screened against the same cell lines. Further investigations showed that EXP57EA activates autophagy and not apoptosis. Various studies on the anticancer effect of artemisinin derivatives have been extensively reported in various cancer cell lines. The next section will attempt to investigate the underlying signaling pathways activated by EXP57EA leading to autophagy.

Various studies have been reported that increased levels of ROS can lead to the induction of autophagy via the JNK pathway, as well as the ER stress pathway through one of its downstream targets PERK (Chen et al. 2009; X. Li et al. 2013). Previous work in our laboratory showed ROS production. In that study, the involvement of O_2^- in mediating the effect of EXP57EA on cancer cells was demonstrated. It was also shown that tempol (a scavenger of O_2^-) inhibited the effect of EXP57EA on cancer cells. In this present study, we wanted to determine the effect of EXP57EA on the PERK/eIF2α/CHOP signaling pathway that has been shown to be triggered by O_2^- production.

WHCO1 cells were plated in 60 mm dishes. After 24 hours, cells were treated with EXP57EA in the presence and absence of tempol. Figure 2.9 shows the effect of EXP57EA on the PERK/eIF2α pathway. WHCO1 cells treated with 5 μM EXP57EA in the presence and absence of tempol did not have any effect on the expression level of p-eIF2α (figure 2.9). In general, the expression level of p-eIF2α was the same in the presence and absence of tempol in WHCO1 cells treated with 5 μM EXP57EA. However, treatment of WHCO1 cells with 15 μM EXP57EA in the absence of tempol stimulated the phosphorylation of eIF2α, but in the presence of tempol, phosphorylation of eIF2α was substantially reduced (figure 2.9).

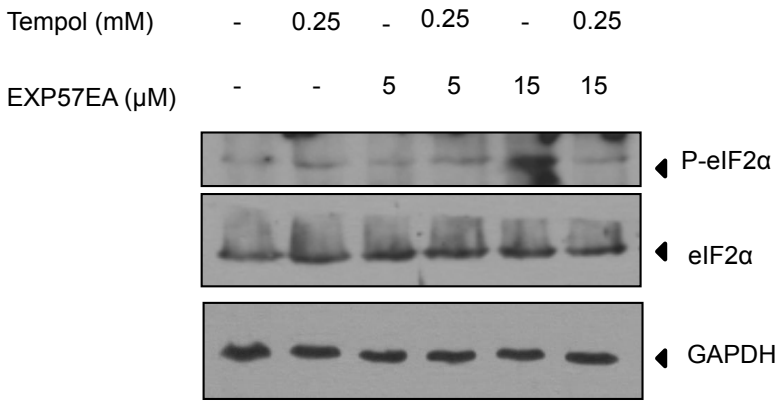

Figure 2.9: The effect of EXP57EA on p-eIF2α level in WHCO1 cells in the presence and absence of tempol. WHCO1 cells were plated at a density of 300000 cells per 60 mm dish. Cells were pre-treated with 0.25 mM tempol or DMSO (control) for 1 hour followed by treatment with 5 μM and 15 μM EXP57EA for 24 hours. Protein was harvested then 40 μg were separated on a 10 % SDS-PAGE and proteins were transferred to a nitrocellulose membrane. The membranes were probed with an antibody recognizing p-eIf2α and total eIf2α. GAPDH was used as a loading control and this figure is representative of two experiments.

PERK is a downstream target of the ER stress pathway that has been reported to be involved in the induction of autophagy through the activation of the transcription factor C/EBP homologous proteins (CHOP) (Shen, Zhang, Wang, et al. 2014b). Consequently, we wanted to see if EXP57EA treatment increases the expression level of CHOP. Real-time PCR (RT-PCR) was used to examine the mRNA expression level of CHOP (standardized to the housekeeping gene GusB) upon EXP57EA treatment. Untreated cells (control) were incubated with DMSO and all the values were relative to the control value. A significant increase in CHOP mRNA expression level was observed in WHCO1, WHCO5, MDA-MB-231 and SiHa cell lines upon 24 hours EXP57EA treatment. However, no significant increase in the mRNA expression level of CHOP was seen in KYSE150 cell line due to discrepancies in Ct values (figure 2.10). Based on these results, it was concluded that CHOP levels were significantly elevated in response to EXP57EA treatment in WHCO1, WHCO5, MDA-MB-231 and SiHa cell lines

but not in KYSE150 cell line (figure 2.10). Figures 2.9 and 2.10 suggested that EXP57EA treatment had an effect on the PERK/eIF2α/CHOP signaling pathway, which has been reported to be involved in the induction of autophagic activity.

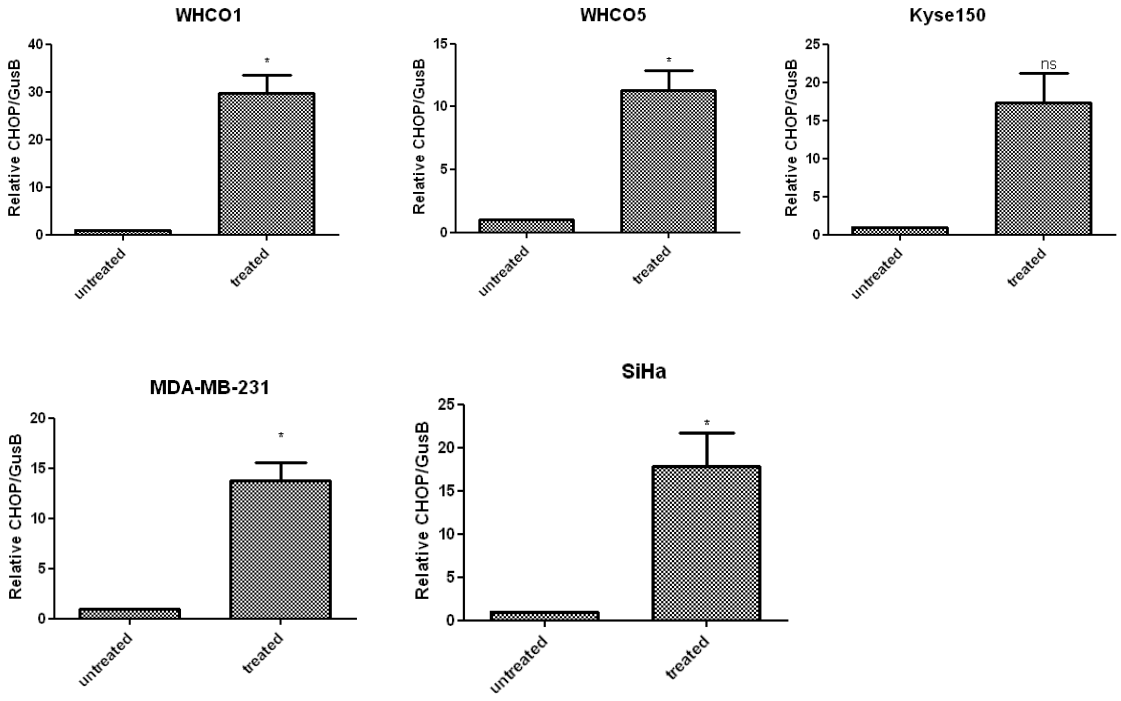

Figure 2.10: Evaluation of mRNA levels of CHOP using quantitative real time RT-PCR. Cells were plated at a density of 80000 cells per 60 mm dish. The cells were treated with 15 µM EXP57EA for 24 hours. RNA was extracted and messenger RNA levels were analyzed by quantitative real time RT-PCR for the gene-encoding CHOP. Results (corrected to GusB) are shown relative to the control cells (untreated) and are represented as the mean ± SD of experiments performed in three independents experiments. $p < 0.05$. ns = non-significant.

Mitogen activating protein kinase (MAPK) signaling pathway has also been implicated in the induction of autophagy (He & Klionsky 2009; Yu et al. 2006). We next determined the effect of EXP57EA on the activation of c-jun N terminal kinase (JNK), a downstream target of MAPK. The treatment of WHCO1 and WHCO5 cells with either 5 µM or 15 µM EXP57EA alone stimulated c-jun phosphorylation and resulted in elevated levels of total c-jun (figure 2.11 and 2.12 respectively). In the presence of the JNK inhibitor SP600125, the expression level of p-c-jun and c-jun decreased in a dose-dependent manner (figure 2.11 and 2.12 respectively). These results showed that the JNK pathway might also be involved in EXP57EA-induced autophagy.

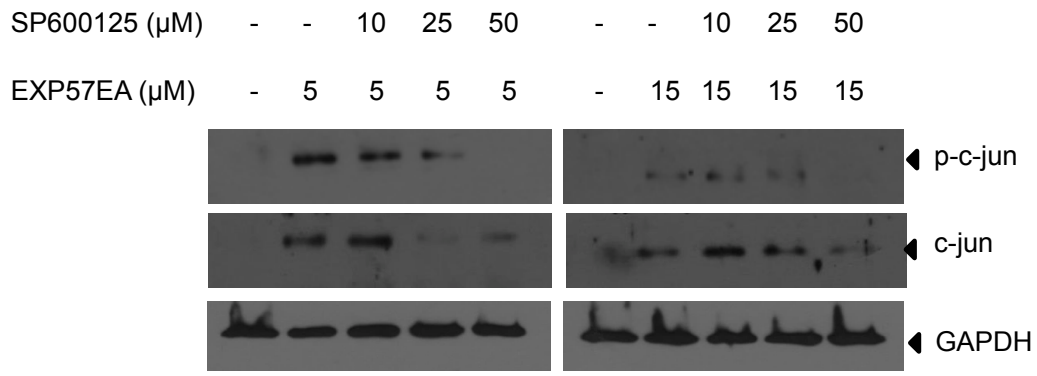

Figure 2.11: The effect of EXP57EA on the expression level of p-c-jun and level of total c-jun in the WHCO1 cell line in the presence and absence of SP600125. WHCO1 cells were plated at a density of 300000 cells per 60 mm dish. Cells were pretreated with 10 μM, 25 μM and 50 μM SP600125 or DMSO for 1 hour followed by treatment with 5 μM and 15 μM EXP57EA for 24 hours. Protein was harvested and 40 μg were separated on a 10 % SDS-PAGE and proteins were transferred to a nitrocellulose membrane. The membrane was probed with antibody recognizing p-c-jun and total c-jun. GAPDH was used as a loading control and this figure is representative of two independent experiments.

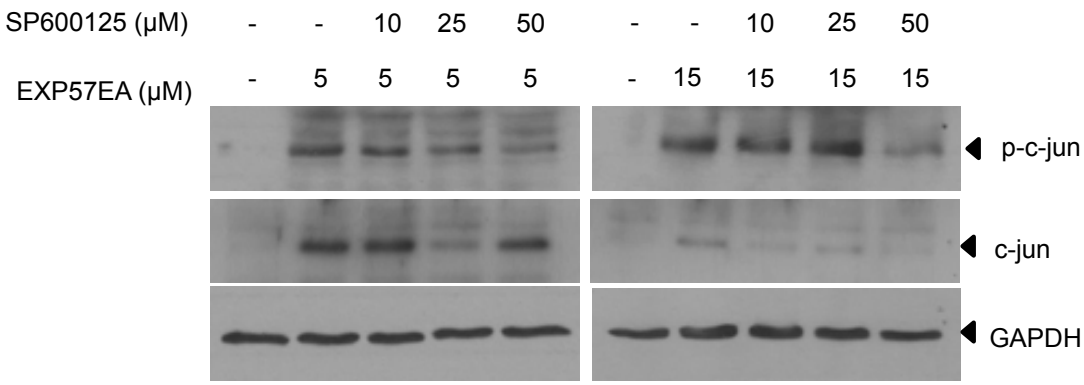

Figure 2.12: The effect of EXP57EA on the expression level of p-c-jun and level of total c-jun in the WHCO5 cell line in the presence and absence of SP600125. WHCO1 cells were plated at a density of 300000 cells per 60 mm dish. Cells were pretreated with 10 μM, 25 μM and 50 μM SP600125 or DMSO for 1 hour followed by treatment with 5 μM and 15 μM EXP57EA for 24 hours. Protein was harvested and 40 μg were separated on a 10 % SDS-PAGE and proteins were transferred to a nitrocellulose membrane. The membrane was probed with antibody recognizing p-c-jun and total c-jun. GAPDH was used as a loading control and this figure is representative of two independent experiments.

CHAPTER 3:

DISCUSSION

Artemisinin and its derivatives have been reported extensively to be good examples of natural product drug discovery considering their role in the treatment of malaria (Cragg & Newman 2005). Moreover, they are also promising lead natural products as many studies have reported their role in the treatment of various cancers as discussed in section 1.2.2. This project took advantage of the potential role of artemisinin as a drug lead by linking the most potent artemisinin like-compound dihydroartemisinin (DHA) with an iodo-isatin azide intermediate compound to form a hybrid compound in order to improve anticancer activity.

In this project the effect of DHA (first generation derivative of artemisinin), cisplatin, a drug currently used for chemotherapy, and the novel hybrid artemisinin compound EXP57EA were assessed on a panel of cancer cell lines. Yde & Issinger et al. 2006 reported that a major drawback of certain compounds such as cisplatin is the severe dose effect on various cancers, which consequently develop resistance to the treatment (Yde & Issinger 2006). This was demonstrated in this study where the IC_{50} values for cisplatin in KYSE150, MDA-MB-231 and SiHa cell lines, were 86 µM, 108.1 µM and 71.1 µM respectively. Moreover, it was also observed that in MDA-MB-231 and SiHa cell lines DHA was not active (NA), unlike WHCO1 and WHCO5 cell lines. A previous study in our laboratory reported that the IC_{50} value of DHA in KYSE150 cell line was 27.9 µM (Shunmoogam-Gounden 2014), whereas in this study DHA was not able to kill KYSE150 cells. It is possible that the KYSE150 cells in the previous study were contaminated with mycoplasma, although mycoplasma assays are routinely conducted in our laboratory. It is difficult to explain this difference, since the EXP57EA had the

same purity profile as previous batches, and the hybrid compound displayed the same biological profile as reported previously. It has been reported that hybrid compounds often display different or better activity than their parental compounds (Teiten et al. 2014). It was shown in this study that the novel hybrid compound EXP57EA was more active with IC_{50} values not exceeding 30 μM across all cell lines, than DHA and cisplatin.

Previous studies have reported the anticancer effect of artemisinin derivatives and demonstrated their ability to induce apoptosis or autophagy in various cancer cell lines (Chen et al. 2014; Du et al. 2013; Hou et al. 2008). Previously in our laboratory, it was shown that the first generation derivative artemisinin compound DHA had a different molecular mechanism of action compared to the novel hybrid compound EXP57EA. It was shown previously in our laboratory that DHA induced apoptosis based on various assays performed on two esophageal cell lines, whereas EXP57EA induced autophagy based on tests performed on the same cell lines.

In this study, the cytotoxic effect of EXP57EA and its parental compound DHA was examined on all cell lines tested. The first part of this study was focused on determining the concentration of DHA and EXP57EA required to kill the cancer cells. Having found the treatment conditions, the effect of these two compounds on cell morphology was investigated (figures 2.3 and 2.4). Cells treated with DHA showed signs of apoptosis such as cell shrinkage. Moreover, PARP was cleaved when the same cells were treated with DHA. These results are consistent with previous results found in our laboratory in WHCO1 cell line (Shunmoogam-Gounden 2014) and also reported by Hou et al. where they demonstrated that DHA and another first generation artemisinin compound (artesunate) induced apoptosis in HepG2 liver cancer cells based on cleaved PARP expression (Hou et al. 2008).

All cells treated with EXP57EA showed no PARP cleavage, consistent with previous results found in our laboratory for the WHCO1 cell line (Shunmoogam-Gounden, 2014). In this study, the inability of EXP57EA to

induce PARP cleavage was observed in a larger panel of cancer cell lines. Here, extensive experimental approaches were also used to show that EXP57EA activated autophagy. These include appearance of vacuoles in cells treated with EXP57EA, analysis of Beclin1 and LC3-II by western blot as well as increased autophagic flux. When all cell lines were treated with EXP57EA, signs of autophagy such as perinuclear vacuoles were observed. A change in the expression level of Beclin1 upon EXP57EA treatment was seen in all cell lines and this suggested that autophagy occurred since Beclin1 is necessary for the induction of autophagy (figure 2.6). Another standard method to show the induction of autophagy is the analysis of LC3-II by western blot. When autophagy occurs, LC3 is cleaved by ATG4 to LC3-I allowing conjugation of LC3-I to PE, generating the lipidated form LC3-II (17 kDa), which is mainly involved in the elongation of the autophagosome structure. Thus LC3-II is a good marker to measure autophagic activity. In this study, we showed that EXP57EA treatment activated LC3-II in all cell lines and this was also suggestive of autophagy (figure 2.7). It was previously demonstrated in our laboratory that EXP57EA increased Beclin1 and LC3-II expression level in WHCO1 and WHCO6 cell lines and this was confirmed in this study for the WHCO1 cell line. Given the novelty of EXP57EA, it has never been reported that this compound increased the expression level of Beclin1 and LC3-II in the other cell lines selected in this study. Various studies have reported that certain compounds caused increased levels of Beclin1 and LC3-II markers in various cancers, which were suggestive of autophagy (Jia et al. 2014; He et al. 2010). However, according to Klionsky et al. 2016, these results are insufficient to conclude that EXP57EA activates autophagy (Klionsky et al. 2016). To determine if a compound truly activates autophagy, one should analyze LC3-II turnover as a marker of autophagic flux by western blot. Autophagic flux refers to the rate of the autophagic process resulting in the degradation of the autolysosomal content (Loos et al. 2014). A study conducted by Jeon et al. demonstrated that 2-deoxyglucose increased autophagic flux in human prostate cancer cells (PC3 cells) (Jeon et al. 2015). Another study showed that Bufalin increased autophagic flux in U87MG and LN229 glioma cell lines (Shen et al. 2014a). In this study two inhibitors NH_4Cl and chloroquine were used and it was found that EXP57EA

increased the autophagic flux in both WHCO1 and SiHa cell lines. Other approaches to show autophagic flux include the use of Bafilomycin A1, pepstatin A and lysosomal proteases such E64d (Klionsky et al. 2016; Zhang et al. 2013). The use of NH_4Cl and chloroquine to inhibit the autophagy process has been reported in various studies (Abdel-Aziz et al. 2014; M. Li et al. 2013) and the data obtained in this study showed that EXP57EA activated the autophagy pathway, resulting in increased LC3-II turnover. Considering that apoptosis is the preferred mode of cell death induced by anti-cancer agents, it was interesting to see that EXP57EA induced a different pathway in all cell lines tested.

Various drugs that have been used for research in various diseases including cancer induce autophagy (Levine et al. 2015). These include, inhibitors of mTOR such as Torin 1 in MEF cells and PP242 in leukemia cells (Thoreen et al. 2009; Janes et al. 2010; Sarkar 2013). Another example of a dug inducing autophagy is the ABT737 4-[4-[[2-(4-chlorophenyl) phenyl]methyl] piperazin-1-yl]-N-[4-[[(2R)-4-(dimethylamino)-1-phenylsulfanylbutan-2-yl]amino]-3-nitrophenyl] sulfonylbenzamide) drug. This drug inhibited the Bcl-2 family of proteins by acting as BH3 mimetic. The latter disrupted the interaction of Bcl-2 and Beclin1 to induce autophagy in Hela cells (Maiuri et al. 2007; Thorburn et al., 2014).

Preliminary evidence in our laboratory showed that EXP57EA activated autophagy through the ER stress pathway via the activation of CHOP in WHCO1 and WHCO6 cell lines. Various studies have linked the PERK/eIF2α/ATF4 unfolded protein response (UPR) signaling pathway to the activation of autophagy via phosphorylated eIF2α-triggered activation of LC3-II in Huntington and Parkinson diseases. A study done by Lugea et al. 2011 and a review by Szegezdi et al. 2006 reported that once ER stress occurs, the first sensor to be activated is PERK. It plays an important in the phosphorylation of eukaryotic translation initiation factor 2α (eIF2α), resulting in the inhibition of protein translation and the activation of two important

autophagy markers such as Autophagy protein 5 (Atg5) and Microtubule-associated light chain 3 (LC3) through activating transcription factor 4 (ATF4) and the C/EBP homologous proteins (CHOP) (Lugea et al. 2011; Szegezdi et al. 2006). In accordance with that, we investigated the effect of EXP57EA on the PERK/eIF2α pathway and the involvement of ROS production in that process. Tempol, a superoxide anion scavenger was used. Tempol is a membrane permeable, metal-independent superoxide dismutase mimetic for superoxide anions. It has been reported that superoxide can be produced by the microsomal monooxygenase (MMO) system of the ER, therefore activating the UPR and resulting in autophagy (Chen et al. 2009). Results of this study showed that EXP57EA treatment alone (15 μM) stimulated phosphorylation of eIF2α. However, in the presence of tempol the level of p-eIF2α decreased significantly (figure 2.9). These results were consistent with a study reported by Jiang et al., 2013 where Selenite stimulated phosphorylation of eIF2α in Jurkat cells (Jiang et al. 2013). Moreover, Dong et al showed that tempol attenuated the expression level of eIF2α in Bovine aortic endothelial cells (BAECs) (Dong et al. 2010).

As mentioned earlier, PERK/eIF2α has been reported to induce autophagy through the activation of CHOP. All cell lines selected in this study were treated with EXP57EA and the results showed an increase in CHOP mRNA expression level except in KYSE150 cell line. These results are consistent with a study done by Shimodaira et al. 2014, where the mRNA expression level of CHOP was elevated in HT29 colon cancer cells treated with thapsigargin (Shimodaira et al. 2014). We concluded that EXP57EA activated the PERK/eIF2α/CHOP pathway. However, further work needs to be done to show that EXP57EA activates autophagic cell death through the PERK/eIF2α/CHOP pathway.

Various signaling pathways have been implicated in autophagic cell death. Among them is the c-Jun NH2-terminal kinase (JNK) pathway (He & Klionsky 2009; Yu et al. 2006). Therefore, we investigated the effect of EXP57EA treatment on p-c-jun and total c-jun levels in WHCO1 and WHCO5 cell lines. Treated cells stimulated phosphorylation of c-jun, however, when a JNK

inhibitor SP600125 was added a dose-dependent decrease of p-c-jun and elevated levels of total c-jun were seen in both cell lines. It has been reported that autophagy was inhibited in IRE1-MEF deficient cells or in cells treated with SP600125, a JNK inhibitor, suggesting that IRE1-JNK is necessary for autophagy and that JNK played an important role in autophagy (Jia et al. 2014; Ogata et al. 2006). In this study, these results suggested that EXP57EA might also play a role in the JNK activation, which has been implicated in autophagic cell death. However, more work needs to be done to characterize the role of JNK in EXP57EA-mediated autophagy.

CHAPTER 4:

CONCLUSION

Cancer represents a major burden worldwide and the number of diagnosed cancer patients has been reported to double by the year 2030. It is well known that diagnosing cancers at an early stage of the disease provides patients with the best possible chance of survival. However, for the present time, there are some cancers that will be diagnosed at a late stage. The mortality rate of this disease could be reduced if improved chemotherapeutic agents could be developed. Effective chemotherapy includes anticancer agents that kill cancer without damaging normal cells. Natural products have proven to be an incredible source of compounds that could be developed into chemotherapeutic agents, therefore the aim of this project was to investigate a novel derivative of a natural product against cancer cells.

This project focused on an artemisinin derivative originally obtained from a plant used in traditional medicine. The novel hybrid compound was synthesized by conjugating the most potent artemisinin compound DHA, with an iodo-isatin intermediate and a novel isatin-artemisinin derivative EXP57EA was generated. In this study it was shown that the novel derivative displayed greater activity than DHA and cisplatin across all cell lines. Moreover, SiHa and MDA-MB-231 cell lines, which have been reported to be resistant, were more sensitive to the novel hybrid compound than its parental compound DHA.

This study investigated some of the effects of EXP57EA. The role of autophagy in cancer is complex since this process has been reported to play a role in cell survival and cell death. In this study, our results showed that EXP57EA activates autophagy since no evidence of apoptosis was seen. Moreover, autophagic flux estimations using ammonium chloride and chloroquine showed that the complete autophagy was activated by

EXP57EA. Various signaling pathways have been implicated in autophagic cell death. In this study, EXP57EA was demonstrated to activate PERK/eIF2α/CHOP as well as the JNK pathways, which have been reported to induce autophagic cell death.

Future work in this study will be done to show that EXP57EA activates autophagy by measuring the autophagic flux in the other cell lines selected for this study. Furthermore, the effect of EXP57EA-induced autophagic cell death through the PERK/eIF2α/CHOP and JNK pathway will also be investigated by analyzing the expression level of LC3-II by western blot. To implicate EXP57EA as a cell death mechanism, it would also be interesting to determine the effect of inhibiting CHOP using siRNA in combination with the JNK inhibitor SP600125 on LC3-II expression levels. It would be very interesting to also determine the effect of the autophagy rescue agents (ammonium chloride, chloroquine, tempol and SP600125) on cell number when treated in combination with EXP57EA.

CHAPTER 5:

MATERIALS AND METHODS

5.1 Cell culture

5.1.1 Cell lines

The esophageal cancer lines WHCO1 and WHCO5 were derived from biopsies of primary esophageal squamous cell carcinomas and kindly provided by Professor Rob Veale (University of Witwatersrand, South Africa) (Shunmoogam-Gounden 2014). The KYSE150 an esophageal squamous cell carcinoma cell line was previously established by Shimada and co-workers (Shimada et al. 1992), was purchased from the German Resource Centre for Biological Material (http://www.dsmz.de). The SiHa cervical cancer cell line and MDA-MB-321 breast cancer cell line were purchased from the American Type Culture collection (Rockville, MD, USA).

5.1.2 Cell Culture

All cell lines were cultured in Dulbecco's Modified Eagles Medium (DMEM) (Invitrogen, USA) supplemented with 100 U/ml penicillin, 100 µg/ml streptomycin and 10% Fetal Bovine Serum (FBS) (Gibco, Paisley, Scotland). Dishes (10 cm) were incubated in a humidified incubator at 37˚C and 5 % CO_2 until 70 % - 80 % confluency was reached.

5.1.3 TrypsinIzation

Once the cells reached 70 % - 80 % confluency, trypsinization was performed as follows:
The DMEM media in dishes was discarded. Thereafter, cells were washed with 5 ml Trypsin- EDTA. The EDTA was discarded and 5 ml of fresh Trypsin-EDTA was added to the dishes to trypsinize the cells. The cells were incubated for 3 min at 37˚C. DMEM media was added to the cells to inactivate the action of trypsin and the cell suspension was transferred in a 12 ml falcon tube and centrifuge at 1000 rpm for 3 min to obtain pellets. The solution containing media and centrifuge was aspirated off and the pellets were resuspended with 5 ml complete DMEM. A fresh 100 mm culture dish was prepared containing 9 ml of fresh media and 1 ml of the resuspended cell was added to the dish.

5.1.4 Mycoplasma Test

Mycoplasma tests were routinely performed to ensure that the cells were not contaminated. Cells were culture in complete DMEM until 60 % - 80 % confluency was reached. Cells were trypsinized as describe in section 5.1.3, however the pelleted cells were resuspended in penicillin and streptomycin free media and plated onto a cover slip. After 24 hours incubation, cells were washed with 1 x PBS and fixed with methanol for 10 min. Fixed cells were further washed with 1 x PBS and stained with DAPI. The cover slip was mount with mowiol 4-88 (Calbiochem#475904) and cells were kept in the dark for 24 hours, following visualization on the phase contrast microscope (Axiovert 200 M microscope (Zeiss)). Images were taken using an Axio CamHR camera with Axiovision software, version 4.7 (Zeiss). Stained nuclei appeared blue and tiny spots in the cytoplasm indicated mycoplasma contamination.

5.2 Compounds and Inhibitors

The two compounds Dyhidroartemisinin (DHA) and EXP57EA were received from the Chemistry Departement, UCT (assessed to be 95 % pure) and dissolved in tissue culture grade DMSO (Sigma-Aldrich® co). Cisplatin, Doxorubicin (DOX), ammonium chloride (NH_4Cl) , chloroquine and JNK inhibitor (SP600125) were were purchased from Sigma-Aldrich® co and dissolved in tissue culture grade DMSO with the exception of Cisplatin and ammonium chloride which were dissolved in 0.9 % saline solution and sterile dH_20 respectively.

5.3 Proliferation assay

Cells were plated at a density of 3 x 10^3 cells/well in a 96 well plate (90 µl per well) and incubated for 24 hours. Treatment of cells included DHA, EXP57EA and Cisplatin at different concentrations. Controls were treated with DMSO. Plated cells were incubated for 48 hours at 37˚C in a CO_2 incubator. Following 48 hours of treatment, 10 µl of MTT reagent (100mg/20ml 1 X PBS) was added to each well before adding the solubilizing reagent and incubated for 4 hours at 37˚C. Absorbance was then measured at 595nm using the plate reader in conjunction with the Gen 5 Data analysis software. The dose response curve was then plotted using PRISM software.

5.4 Western blot analysis

5.4.1 Plating of cells

All cell lines were cultured and trypisinized as described in section 5.1.3. The cells were counted using a haemocytometer. The cells were plated in 6 cm dishes at a cell density of 0.75 x 10^5 cells/dish. The dishes were placed in a

CO_2 incubator overnight. Treatment was done using the same drugs mentioned in section 5.3.

5.4.2 Protein extraction

Following treatment of cells on dishes with the desired compound, media was transferred to a 12 ml tube and kept on ice. Cells were washed with 1 X PBS and the PBS wash was added to the originally collected media. Cells were centrifuged at 10000 rpm for 5 min at room temperature. Pellets were resuspended with 60 µl of a cocktail containing radioimmunoprecipitation assay buffer (RIPA) (150 mM NaCl, Triton X-100, 0.5% Sodium deoxycholate, 0.1% SDS and 50 mM Tris), 1 X protease inhibitors (Sigma, USA) 1 mM Sodium orthovanadate (Na_3V0_4) and 1 mM Sodium Fluoride (NaF) were added. The cocktail was added to the dishes and cells were scraped off using a cell scraper. Cell lysates were mixed with the resupended pellets and sonicated for 5 sec on ice. Cells were then centrifuged at 4˚C for 5min at 10000 rpm. The supernatant was transferred to a new microcentrifuge tube and proteins were quantified using the BCA (Bicinchoninic Acid) assay kit (Pierce Thermo Scientific, USA). Absorbance was measured at 595nm and proteins concentrations were determined using a set of BSA standards.

5.4.3 SDS-PAGE

Proteins samples were prepared by the addition of 6 X loading dye. The final volume was made up with RIPA buffer. Samples were heated at 90˚C for 5 min to denature proteins. Proteins (20 µg or 40 µg) were loaded onto a 10% polyacrylamide gel and electrophoresed at 160 V for approximately 1 hour in 1 X running buffer. Proteins within the gel were transferred onto a nitrocellulose membrane at 100 V for 70 min in 1 X transfer buffer.

5.4.4 Membrane probing

After transfer, the membrane was blocked in 5% milk powder (Elite fat free instant milk powder) with TBST (TBS Tween) for 1 hour 30 min at room temperature with gentle shaking. After blocking, the membrane was briefly washed with TBST. The membrane was probed with primary antibodies (see table 1) and the membrane left overnight at 4˚C with agitation. Following incubation, the membrane was washed three times with TBST for 5 min each and incubated with secondary antibodies for 1 hour at room temperature with gentle shaking. Finally the membrane was washed once again three times with TBST.

Table 5.1: Antibodies concentrations and incubations conditions

Primary antibody	Primary antibody condition	Secondary antibody	Primary antibody condition	Substrates
Parp -1/2 (H-250) [sc-7150, Santa Cruz Biotechnology]	1:1000 in TBST	Goat anti-rabbit [Bio-Rad]	1:5000 in TBST	LumiGlo® chemiluminescent system (KPL)
BECN1 (E-8) [sc-48341, Santa Cruz Biotechnology]	1:2000 in 5 % Milk-TBST	Goat anti-mouse [Bio-Rad]	1:5000 in 5 % Milk-TBST	Clarity™ Western ECL substrate
GAPDH (0411) [sc-47724, Santa Cruz Biotechnology]	1:10000 in 5 % Milk- TBST	Goat anti-mouse [Bio-Rad]	1:5000 in 5 % Milk-TBST	LumiGlo® chemiluminescent system (KPL)
LC3B (2775S) cell signaling	1:250 in 5 % BSA-TBST	Goat anti-rabbit [Bio-Rad]	1:2500 in 5 % Milk-TBST	Clarity™ Western ECL substrate
Anti p-cjun (ser 63/73) [sc-16312, Santa Cruz Biotechnology]	1:500 in 5 % BSA-TBST	Goat anti-rabbit [Bio-Rad]	1:1000 in 5 % Milk-TBST	Clarity™ Western ECL substrate
Anti cjun (H79) [sc-1694, Santa Cruz Biotechnology	1:1000 in 5 % BSA-TBST	Goat anti-rabbit [Bio-Rad]	1:2500 in 5 % Milk-TBST	Clarity™ Western ECL substrate
P-eIF2α [sc-101670, Santa Cruz Biotechnology	1:500 in 5 % Milk-TBST	Goat anti-rabbit [Bio-Rad]	1:2500 in 5 % Milk-TBST	Clarity™ Western ECL substrate
eIF2α [sc-11386, Santa Cruz Biotechnology	1:500 in 5 % Milk-TBST	Goat anti-rabbit [Bio-Rad]	1:5000 in 5 % Milk-TBST	Clarity™ Western ECL substrate

5.4.5 Immunodetection

Proteins bands were detected using LumiGLO, a lumino-based chemiluminescent substrate (KPL, USA) or Clarity™ Western ECL substrate. The membrane was incubated with equal volume of substrate A and B for 1 min and 5 min for LumiGLO, a lumino-based chemiluminescent substrate (KPL, USA) or Clarity™ Western ECL substrate respectively. The membrane

was then exposed to X-ray film for the desired time. The x-ray film was developed until the bands of interest appeared.

5.4.6 Membrane striping

Membrane could be reprobed with different antibodies following stripping. Membranes were stripped with 10 % acetic acid (see appendix) for 10 min at room temperature with gentle shaking. Following stripping, membranes were washed 3 times with TBST for 5 min each at room temperature with gentle shaking. The membranes were then blocked and probed as above (section 5.4.4) according to the antibody condition.

5.5 RNA extraction, quantification and preparation for real-time PCR

5.5.1 RNA extraction from cultured cells

In order to extract RNA, 3 ml of complete media containing 8 x 10^4 cells were plated in 60 mm dishes and incubated for 24 hours, after which cells were treated with 15 µM of EXP57EA for 24 hours. RNA was harvested from each dish with QIAzol (300 µl per 3 ml) (Qiagen, Germany). Briefly, cells were washed twice with ice cold 1 x PBS, after which QIAzol was added to cells and incubated for 5 min at room temperature. RNA was then scraped off using a cell scraper and transferred to a chilled eppendorf tube. Subsequently, 60 µl of Chloroform per 1 ml of QIAzol was added to each sample, mixed vigorously for 15 s followed by 2-3 min incubation at room temperature. The samples were centrifuged at 12000 x g at 4˚C for 15 min in order to separate the two phases. The upper aqueous phase was transferred to a clean tube and RNA was precipitated using 150 µl isopropanol (1/2 volume of QIAzol) and the tubes were inverted gently. This was followed by 10 min incubation at room temperature and the samples were centrifuged at 12000 x g at 4˚C for 10 min. The supernatant was discarded and RNA pellets were washed with 70 % ethanol followed by centrifugation at 12000 x g (4˚C) for 5 min. The supernatant was discarded and the RNA pellets were air-dried

for 15-20 min and the pellet were resuspended with 30 µl diethylpyrocarbonate (DEPC) - treated water. DEPC-treated water was prepared by thoroughly dissolving 1 ml of DEPC in 1 L of distilled water (0.1 % DEPC-treated water). After an overnight incubation, the DEPC-treated water was autoclaved.

5.5.2 Quantification

RNA was quantified using the Nanodrop^{TM} 2000c spectrophotometer (Thermo Scientific, USA) and 2 µg was mixed with RNA loading dye (containing 0.5 µg/ml ethidium bromide) and electrophoresed on a 1.5 % MOPS/formaldehyde agarose gel to see if the extracted RNA were contaminated.

5.5.3 cDNA synthesis

cDNA was prepared by mixing 3 µg of the total RNA with a desired volume of DEPC-dH_20 and 0.5 µg (1µl) of oligo-$(dT)_{20}$ primer (Promega, USA) was added to a final volume of 9 µl. The two samples were placed at 70˚C for 5 min following incubation on ice for 5 min. Subsequently, 1 µl ImPromII Reverse Transcriptase II, 40 units of RNAsin RNase inhibitor, 1.2 mM $MgCl_2$, 5 x reaction buffer and 3.3 mM dNTPs (all reagents were purchased from Promega, USA) were added to each sample to a final volume of 20 µl. The sample were incubated at RT for 5 min, 42˚C for 1 hour, 70˚C for 15 min and the resultant cDNA was placed on ice until use for quantitative real-time PCR or store at -80° C.

5.5.4 Quantitative real-time PCR

Quantitative real time reverse transcription polymerase chain reaction was performed using the StepOne Real-time PCR system (Applied Biosystems, USA), and the comparative threshold cycle (C_T) method was used to analyse values generated. Real-time PCR was performed using the KAPA SYBR Qpcr master mix. 20 µM of the housekeeping gene's primers GusB or 10 µM of the gene of interest's primers CHOP were added to 2 µl cDNA and 2 µl

DEPC-treated water was use as Positive control. *Gus* B forward primer was 5- CTC-ATT-TGG-AAT-TTT-GCC-GAT -3'. Reverse: 5'- CCG-AGT-GAA-GAT-CCC-CTT TTT –'3. CHOP forward primer was 5'- ACC- TCC-THGG An AAA-TGA- AGA GGGA- AG -
,3 and the reverse primer was 5 % TCT-CCT- TCA0TGC-GCT-GCT-TT-3mM. The PCR cycling conditions were 95˚C for 3 min followed by 40 cycles of denaturation at 95˚C for 1 s, annealing at 60˚C (GusB and CHOP primers) for 20 s and finally 95˚C for 15 s. C_T values were calculated using StepOne Version 2.0 software (Applied Biosystems) and the Delta Delta C_T method was used to calculate the expression of target mRNA relative to that of the housekeeping gene, either *β-glucuronidase* (GusB) or Glyceraldehyde 3-phosphate dehydrogenase (GADPH). PCR products were electrophoresed on a 2 % gel to ensure that single specific PCR product was amplified and that there was no contamination or primer-dimer formation. Samples were mixed with 6 x loading dye and electrophoresed at 80 V for 1 hour. A DNA ladder (O'GeneRuler DNA Ladder Mix) was used to determine the size of the targeted amplicon

BIBLIOGRAPHY

Abdel-Aziz, A.K. et al. Chloroquine synergizes sunitinib cytotoxicity via modulating autophagic, apoptotic and angiogenic machineries. *Chemico-Biological Interactions* **217**, 28–40 (2014).

Aita, V.M. et al. Cloning and genomic organization of beclin 1, a candidate tumor suppressor gene on chromosome 17q21. *Genomics* **59**, 59–65 (1999).

Alessi, D.R. et al. Characterization of a 3-phosphoinositide-dependent protein kinase which phosphorylates and activates protein kinase Balpha. *Current Biology* **7**, 4261–269 (1997).

Andrew Thorburn, Douglas H. Thamm, and Daniel L.Gustafson. Autophagy and Cancer. *Molecular pharmacology* **85**, 830–838 (2014).

Annunziato, L. et al. Apoptosis induced in neuronal cells by oxidative stress: role played by caspases and intracellular calcium ions. *Toxicology Letters* **139**, 125–133(2003).

Arico, S. et al. The Tumor Suppressor PTEN Positively Regulates Macroautophagy by Inhibiting the Phosphatidylinositol 3-Kinase/Protein Kinase B Pathway. *Journal of Biological Chemistry* **276**, 35243–35246 (2001).

Aronson, L.I. & Davies, F.E. DangER: Protein ovERload. Targeting protein degradation to treat myeloma. *Haematologica* **97**, 1119–1130 (2012).

Ashton, M. et al. Artemisinin kinetics and dynamics during oral and rectal treatment of uncomplicated malaria. *Clinical Pharmacology and Therapeutics* **63**, 482–493 (1998).

Baudet, C. et al. Differentially expressed genes in C6.9 glioma cells during vitamin D-induced cell death program. *Cell death and differentiation* **5**, 116–125 (1998).

Beaglehole, R. et al. Priority actions for the non-communicable disease crisis. *The Lancet* **377**, 1438–1447 (2011).

Beekman, A.C. et al. Cytotoxicity of artemisinin, a dimer of dihydroartemisinin, artemisitene and eupatoriopicrin as evaluated by the MTT and clonogenic assay. *Phytotherapy Research* **10**, 140–144 (1996).

Berry, D. a et al. Effect of screening and adjuvant therapy on mortality from breast cancer. *The New England journal of medicine* **353**, 1784–1792 (2005).

Bhanot et al. Natural sources as potential anti-cancer agents. *International*

Journal of Phytomedecine **3**, 9–26 (2011).

Bialik, S. et al. Systems biology analysis of programmed cell death. *Trends in Biochemical Sciences* **35**, 556–564 (2010).

Bommer, U.A. & Thiele, B.J. The translationally controlled tumour protein (TCTP). *International Journal of Biochemistry and Cell Biology* **36**, 379–385 (2004).

Bostwick, D.G. et al. Antioxidant enzyme expression and reactive oxygen species damage in prostatic intraepithelial neoplasia and cancer. *Cancer* **89**, 123–134 (2000).

Boujrad, H. et al. AIF-mediated programmed necrosis: A highly regulated way to die. *Cell Cycle* **6**, 2612–2619 (2007).

Brech, A. et al. Autophagy in tumour suppression and promotion. *Molecular Oncology* **3**, 366–375 (2009).

Brüne, B. Nitric oxide: NO apoptosis or turning it ON? *Cell death and differentiation* **10**, 864–869 (2003).

Bustos, M.D.G., Gay, F. & Diquet, B. In-vitro tests on Philippine isolates of Plasmodium falciparum against four standard antimalarials and four qinghaosu derivatives. *Bulletin of the World Health Organization* **72**, 729–735 (1994).

Casao, A. et al. Cleaved PARP-1, an Apoptotic Marker, can be Detected in Ram Spermatozoa. *Reproduction in Domestic Animals* **50** 688–691(2015).

Chaitanya, G. V, Steven, A.J. & Babu, P.P PARP-1 cleavage fragments: signatures of cell-death proteases in neurodegeneration. *Cell Communication and Signalingl* **8,** 31 (2010).

Chen, N. & Karantza-Wadsworth, V. Role and regulation of autophagy in cancer. *Biochimica et Biophysica Acta - Molecular Cell Research* **1793**, 1516–1523 (2009).

Chen, L. et al. Autophagy inhibition contributes to the synergistic interaction between EGCG and doxorubicin to kill the hepatoma Hep3B cells. *PloS one* **9**, p.e85771 (2014).

Chen, N. & Karantza-Wadsworth, V. Role and regulation of autophagy in cancer. *Biochimica et Biophysica Acta - Molecular Cell Research* **1793**, 1516–1523 (2009).

Chen, S. et al. Autophagy is a therapeutic target in anticancer drug resistance. *Biochimica et biophysica acta* **1806**, 220–229 (2010).

Chen, Y. et al. Oxidative stress induces autophagic cell death independent of apoptosis in transformed and cancer cells. *Cell death and differentiation* **15**, 171–182 (2008).

Cragg, G.M. et al. The taxol supply crisis. New NCI policies for handling the large-scale production of novel natural product anticancer and anti-HIV agents. *Journal of natural products* **56**, 1657–1668 (1993).

Cragg, G.M. & Newman, D.J. Plants as a source of anti-cancer agents. *Journal of Ethnopharmacology* **100**, 72–79 (2005).

Creek, D.J. et al. Relationship between antimalarial activity and heme alkylation for spiro- and dispiro-1,2,4-trioxolane antimalarials. *Antimicrobial Agents and Chemotherapy* **52**, 1291–1296 (2008).

Crespo-Ortiz, M.P. & Wei, M.Q. Antitumor activity of artemisinin and its derivatives: From a well-known antimalarial agent to a potential anticancer drug. *Journal of Biomedicine and Biotechnology* (2012).

Darby, S. et al. Radon in homes and risk of lung cancer: collaborative analysis of individual data from 13 European case-control studies. *BMJ (Clinical research ed.)* **330**, 223 (2005).

Das, A.K. Anticancer effect of antimalarial artemisinin compounds. *Annals of medical and health sciences research* **5**, 93–102 (2015).

Debatin, K.-M. & Krammer, P.H. Death receptors in chemotherapy and cancer. *Oncogene* **23**, 2950–2966 (2004).

Ding, W.-X. et al. Linking of autophagy to ubiquitin-proteasome system is important for the regulation of endoplasmic reticulum stress and cell viability. *The American journal of pathology* **171**, 513–24 (2007).

Dong, Y. et al., Activation of AMP-activated protein kinase inhibits oxidized LDL-triggered endoplasmic reticulum stress in vivo. *Diabetes* **59**, 1386–1396 (2010).

Du, J.H. et al. Artesunate induces oncosis-like cell death in vitro and has antitumor activity against pancreatic cancer xenografts in vivo. *Cancer Chemotherapy and Pharmacology* **65**, 895–902 (2010).

Du, X.-X. et al. Initiation of apoptosis, cell cycle arrest and autophagy of esophageal cancer cells by dihydroartemisinin. *Biomedicine & pharmacotherapy = Biomédecine & pharmacothérapie* **67**, 417–424 (2013).

Efferth, T. et al. Molecular modes of action of artesunate in tumor cell lines. *Molecular pharmacology* **64**, 382–394 (2003).

Enzinger, P.C. & Mayer, R.J. Esophageal cancer. *The New England journal of medicine* **349**, 2241–2252 (2003).

Fang, W.-S. & Liang, X.-T. Recent progress in structure activity relationship and mechanistic studies of taxol analogues. *Mini reviews in medicinal chemistry* **5**, 1–12 (2005).

Firestone, G.L. & Sundar, S.N. Anticancer activities of artemisinin and its bioactive derivatives. *Expert reviews in molecular medicine* **11**, p.e32 (2009).

Freedman, R.A. et al. Receipt of locoregional therapy among young women with breast cancer. *Breast Cancer Research and Treatment* **135**, 893–906 (2012).

French, L.E. & Tschopp, J. Protein-based therapeutic approaches targeting death receptors. *Cell death and differentiation* **10**, 117–123 (2003).

Fuchs, C., Mitchell, E.P. & Hoff, P.M. Irinotecan in the treatment of colorectal cancer. *Cancer Treatment Reviews* **32**, 491–503 (2006).

Fujita, E. et al. Two endoplasmic reticulum-associated degradation (ERAD) systems for the novel variant of the mutant dysferlin: Ubiquitin/proteasome ERAD(I) and autophagy/lysosome ERAD(II). *Human Molecular Genetics* **16**, 618–629 (2007).

Fulda, S. & Debatin, K. Caspase Activation in Cancer Therapy Caspases as Central Death Effector Molecules Pathways of Caspase Activation Signaling Pathways in Cancer Therapy. 13–18 (2013).

Fulda, S. & Pervaiz, S. Apoptosis signaling in cancer stem cells. *The international journal of biochemistry & cell biology* **42**, 31–38 (2010).

Geng, J. & Klionsky, D.J. Quantitative regulation of vesicle formation in yeast nonspecific autophagy. *Autophagy* **4**, 955–957(2008).

Gordaliza, M. Natural products as leads to anticancer drugs. *Clinical and Translational Oncology* **9**, 767–776 (2007).

Gottesman, M.M. Carcinoma oesophagus. *Structure of a multidrug transporter: Crystal structures of a mammalian multidrug efflux pump bound to peptide inhibitors may reveal drug binding sites*. 32–34 (2009).

Gottlieb, R.A. et al. Untangling autophagy measurements all fluxed up. *Circulation Research* **116**, 504–514 (2015).

Gravett, A.M. et al. In vitro study of the anti-cancer effects of artemisone alone or in combination with other chemotherapeutic agents. *Cancer Chemotherapy and Pharmacology* **67**, 569–577 (2011).

Gukovskaya, a. S. & Gukovsky, I. Autophagy and pancreatitis. *AJP: Gastrointestinal and Liver Physiology* **303**, G993–G1003 (2012).

Gutierrez, M.G. et al., 2004. Rab7 is required for the normal progression of the autophagic pathway in mammalian cells. *Journal of cell science*, 117, pp.2687–2697.

Gutierrez, M.G. et al. Rab7 is required for the normal progression of the autophagic pathway in mammalian cells. *Journal of cell science* **117**, 2687–2697 (2004).

Gwinn, D.M. et al. AMPK phosophorylation of raptor mediates a metabollic checkpoint. *Molecular Cell* **30**, 14–226 (2008).

Hait, W.N. et al. Tubulin Targeting Agents. *Update on Cancer Therapeutics* **2**, 1–18 (2007).

Hamacher-Brady, A. et al. Artesunate activates mitochondrial apoptosis in breast cancer cells via iron-catalyzed lysosomal reactive oxygen species production. *Journal of Biological Chemistry* **286**, 6587–6601 (2011).

Hanahan, D. & Weinberg, R.A. Hallmarks of cancer: The next generation. *Cell* **144**, 646–674 (2011).

Haynes, R. et al. C-10 Ester and Ether Derivatives of Dihydroartemisinin− 10‑α Artesunate, Preparation of Authentic 10‑β Artesunate, and of Other Ester and Ether Derivatives Bearing Potential Aromatic Intercalating Groups at C-10. *European Journal of Organic Chemistry,* 113–132 (2002).

He Karakaş & D & Gözüaçik. Autophagy and cancer. *Turkish Journal of Biology* **38**, 720–739 (2014).

He, C. & Klionsky, D.J. Regulation Mechanisms and Signalling Pathways of Autophagy. *Annual review of genetics* **43**, 67 (2009).

He, Q. et al. Dihydroartemisinin upregulates death receptor 5 expression and cooperates with TRAIL to induce apoptosis in human prostate cancer cells. *Cancer biology & therapy* **9**, 819–824 (2010).

Hengartner, M.O. The biochemistry of apoptosis. *Nature* **407**, 770–776 (2000).

Hou, J. et al. Experimental therapy of hepatoma with artemisinin and its derivatives: in vitro and in vivo activity, chemosensitization, and mechanisms of action. *Clinical cancer research : an official journal of the American Association for Cancer Research* **14**, 5519–5530 (2008).

Høyer-Hansen, M. et al. Control of Macroautophagy by Calcium, Calmodulin-Dependent Kinase Kinase-β, and Bcl-2. *Molecular Cell* **25**, 193–205 (2007).

Høyer-Hansen, M. & Jäättelä, M. AMP-activated protein kinase: A universal regulator of autophagy? *Autophagy* **3**, 381–383 (2007).

Hsu, E. Reflections on the “discovery” of the antimalarial qinghao. *British Journal of Clinical Pharmacology* **61**, 666–670 (2006).

Inguscio, V., Panzarini, E. & Dini, L. Autophagy Contributes to the Death/Survival Balance in Cancer PhotoDynamic Therapy. *Cells* **1**, 464–491 (2012).

Inoki, K., Zhu, T. & Guan, K.-L. TSC2 mediates cellular energy response to control cell growth and survival. *Cell* **115**, 577–590 (2003).

Ionov, Y. et al. Manipulation of nonsense mediated decay identifies gene mutations in colon cancer Cells with microsatellite instability. *Oncogene* **23**, 639–645 (2004).

Jackson, S. & Seaman, M. Inductionof autophagy and inhibition of tumorigenesis by beclin1. *Nature* **402,** 1–5 (1999).

Janes, M.R. et al. Effective and selective targeting of Ph+ leukemia cells using a TORC1/2 kinase inhibitor. *Nature Medicine* **16**, 205–213 (2010).

Jefford, C.W. New developments in synthetic peroxidic drugs as artemisinin mimics. *Drug Discovery Today* **12**, 487–495 (2007).

Jeon, J.Y. et al. The bifunctional autophagic flux by 2-deoxyglucose to control survival or growth of prostate cancer cells. *BMC cancer* **15**, 623 (2015).

Jia, G. et al. The activation of c-Jun NH_2-terminal kinase is required for dihydroartemisinin-induced autophagy in pancreatic cancer cells. *Journal of experimental & clinical cancer research* **33,** 8 (2014).

Jiang, Q. et al. ATF4 activation by the p38MAPK-eIF4E axis mediates apoptosis and autophagy induced by selenite in Jurkat cells. *FEBS letters* **587**, 2420–2429 (2013).

Jiao, Y. et al. Dihydroartemisinin is an inhibitor of ovarian cancer cell growth. *Acta pharmacologica Sinica* **28**, 1045–1056 (2007).

Johnson, D.G. & Walker, C.L. Cyclins and Cell Cycle Checkpoints. *Annual Review of Pharmacology and Toxicology* **39**, 295–312 (1999).

Klionsky DJ et al. Guidelines for use and interpretation of assays for monitoring autophagy (3rd edition). *Autophagy* **12**,1–222 (2016).

Klionsky, D.J. The molecular machinery of autophagy: unanswered questions. *Journal of Cell Science* **118**, 7–18 (2005).

Klionsky, D.J. & Emr, S.D. Autophagy as a regulated pathway of cellular degradation. *Science (New York, N.Y.)* **290**, 1717–1721 (2000).

Komatsu, M. et al. Impairment of starvation-induced and constitutive autophagy in Atg7-deficient mice. *Journal of Cell Biology* **169**, 425–434 (2005) .

Lai, H. et al. Artemisinin-transferrin conjugate retards growth of breast tumors in the rat. *Anticancer Research* **29**, 3807–3810 (2009).

Lai, H. & Singh, N.P. Selective cancer cell cytotoxicity from exposure to dihydroartemisinin and holotransferrin. *Cancer Letters* **91**, 41–46 (1995).

Lavrik, I., Golks, A. & Krammer, P.H. Death receptor signaling. *Journal of Cell Science* **118**, 265–267 (2005) .

Levine, B. Q & A Autophagy and cancer. *Nature* **446**, 745–747 (2007).

Levine, B. & Klionsky, D.J. Development by Self-DigestionMolecular Mechanisms and Biological Functions of Autophagy. *Developmental Cell* **6**, 463–477 (2004).

Levine, B., Packer, M. & Codogno, P. Development of autophagy inducers in clinical medicine. *Journal of Clinical Investigation* **125**, 14–24 (2015).

Li, M. et al. Suppression of lysosome function induces autophagy via a feedback down-regulation of MTOR complex 1 (MTORC1) activity. *Journal of Biological Chemistry* **288**, 35769–35780 (2013).

Li, X. et al. Beclin1 inhibition promotes autophagy and decreases gemcitabine–induced apoptosis in Miapaca2 pancreatic cancer cells. *Cancer Cell International* **13**, p.1 (2013).

Li, X., Zhang, K. & Li, Z. Unfolded protein response in cancer: the physician's perspective. *Journal of hematology & oncology*, **4**, 8 (2011) .

Liu, J. jie et al. Targeting apoptotic and autophagic pathways for cancer therapeutics. *Cancer Letters* **300**, 105–114 (2011).

Liu, L.F. et al. Mechanism of Action of Camptothecin. *Annals of the New York Academy of Sciences* **922**, 1–10 (2006).

Liu, Y. & Levine, B. Autosis and autophagic cell death: the dark side of autophagy. *Cell death and differentiation* **22**, 367–376 (2015).

Lock, R. & Debnath, J. Extracellular matrix regulation of autophagy. *Current Opinion in Cell Biology* **20**, 583–588 (2008).

Loos, B., du Toit, A. & Hofmeyr, J.-H.S. Defining and measuring autophagosome flux—concept and reality. *Autophagy* **10**, 2087–2096 (2014).

Lu, J.J. et al. Dihydroartemisinin accelerates c-MYC oncoprotein degradation

and induces apoptosis in c-MYC-overexpressing tumor cells. *Biochemical Pharmacology* **80**, 22–30 (2010).

Lu, J.J. et al. The anti-cancer activity of dihydroartemisinin is associated with induction of iron-dependent endoplasmic reticulum stress in colorectal carcinoma HCT116 cells. *Investigational New Drugs* **29**, 1276–1283 (2011).

Lu, Y.-Y. et al. Single-cell analysis of dihydroartemisinin-induced apoptosis through reactive oxygen species-mediated caspase-8 activation and mitochondrial pathway in ASTC-a-1 cells using fluorescence imaging techniques. *Journal of biomedical optics* **15**, p.046028 (2014).

Lu, Y.Y. et al. Dihydroartemisinin (DHA) induces caspase-3-dependent apoptosis in human lung adenocarcinoma ASTC-a-1 cells. *Journal of Biomedical Science* **16**, 16 (2009).

Lugea, A. et al. Adaptive unfolded protein response attenuates alcohol-induced pancreatic damage. *Gastroenterology*, **140**, 987–997 (2011).

Machiels, Jean Pascal, Lambretcht, M., Hanin, F-X., Gregoire, V., Schmitz, S., & hamoir M. Advances in the management of squamous cell carcinoma of the head and neck. *F1000Prime Reports* **6**, 1–10 (2014).

Maiuri, M.C. et al. Functional and physical interaction between Bcl-X(L) and a BH3-like domain in Beclin-1. *The EMBO journal* **26**, 2527–2539 (2007).

Mashima, T. & Tsuruo, T. Defects of the apoptotic pathway as therapeutic target against cancer. *Drug Resistance Updates* **8**, 339–343 (2005).

Mathew, R., Karantza-Wadsworth, V. & White, E. Role of autophagy in cancer. *Nature reviews. Cancer* **7**, 961–967 (2007).

Maude, R.J., Woodrow, C.J. & White, L.J. Artemisinin antimalarials: Preserving the “magic bullet.” *Drug Development Research* **71**, 12–19 (2010).

McCall, K. Genetic control of necrosis-another type of programmed cell death. *Current Opinion in Cell Biology* **22**, 882–888 (2010).

McCormack, V.A. & Schüz, J. Africa’s growing cancer burden: Environmental and occupational contributions. *Cancer Epidemiology* **36**, 1–7 (2012).

Meijer, A.J. & Codogno, P. Regulation and role of autophagy in mammalian cells. *International Journal of Biochemistry and Cell Biology* **36**, 2445–2462 (2004).

Mercer, A.E. et al. Evidence for the involvement of carbon-centered radicals in the induction of apoptotic cell death by artemisinin compounds. *Journal of Biological Chemistry* **282**, 9372–9382 (2007).

Mercer, A.E. et al. The role of heme and the mitochondrion in the chemical and molecular mechanisms of mammalian cell death induced by the artemisinin antimalarials. *Journal of Biological Chemistry* **286**, 987–996 (2011) .

Meunier, B., Robert, A. & Spectus, C.O.N. Heme as trigger and target for trioxane-containing Antimalarial Drugs. *Accounts of Chemical Research* **43**, 1444-1451 (2010).

Miracco, C. et al. Protein and mRNA expression of autophagy gene Beclin 1 in human brain tumours. *International Journal of Oncology*, **30**, 429–436 (2007).

Mizushima, N. et al. Mouse Apg16L, a novel WD-repeat protein, targets to the autophagic isolation membrane with the Apg12-Apg5 conjugate. *Journal of cell science* **116**, 1679–1688 (2003).

Mizushima, N. & Komatsu, M. Autophagy: Renovation of cells and tissues. *Cell* **147**, 728–741 (2011).

Mizushima, N., Noda, T. & Ohsumi, Y. Apg16p is required for the function of the Apg12p-Apg5p conjugate in the yeast autophagy pathway. *EMBO Journal*, **18,** 3888–3896 (1999).

Mizushima, N. & Yoshimori, T. How to Interpret LC3 Immunoblotting ND RIB ND ES SC RIB. *Autophagy*, **3**, 4–7 (2007).

Mizushima, N., Yoshimorim, T. & Levine, B. *Cell* **140**, 13–326 (2010).

Moten, A. et al. Improving cancer care in developing settings. *Journal of global health* **4**, 1–5 (2014).

Nakatogawa, H. et al. Atg4 recycles inappropriately lipidated Atg8 to promote autophagosome biogenesis. *Autophagy* **8**, 177–186 (2012).

Newman, D.J., Cragg, G.M. & Snader, K.M. The influence of natural products upon drug discovery. *Natural product reports* **17**, 215–234 (2000).

Nirmala, M.J., Samundeeswari, a. & Sankar, P.D. Natural plant resources in anti-cancer therapy-A review. *Research in Plant Biology* **1**, 1–14 (2011).

Nishida, K., Yamaguchi, O. & Otsu, K. Crosstalk between autophagy and apoptosis in heart disease. *Circulation Research* **103**, 343–351 (2008).

Noori, S. & Hassan, Z.M. Dihydroartemisinin shift the immune response towards Th1, inhibit the tumor growth in vitro and in vivo. *Cellular immunology* **271**, 67–72 (2011).

O'Neill, P.M., Barton, V.E. & Ward, S.A. The molecular mechanism of action of artemisinin - The debate continues. *Molecules* **15**, 1705–1721 (2010).

Ogata, M. et al. Autophagy is activated for cell survival after endoplasmic reticulum stress. *Molecular and Cell Biology*, **26**, 9220–9231 (2006).

Ohsumi, Y et al. Tor-mediated induction of autophagy via an Apg1 protein kinase complex. *Journal of Cell Biology* **150,** 1507–1513 (2000).

Ohsumi, Y. & Mizushima, N. Two ubiquitin-like conjugation systems essential for autophagy. *Seminars in Cell and Developmental Biology* **15**, 231–236 (2004).

Ojima, I. et al. Syntheses and Biological Activity of C-3-difluoromethyl-Taxoids. *Bioorganic and Medicinal Chemistry* **8**,1619–1628 (2000).

Olliaro, P.L. et al. Drug studies in developing countries. 894–895 (2001).

Orfanelli, T. et al. Involvement of autophagy in cervical, endometrial and ovarian cancer. *International Journal of Cancer* **135**, 519–528 (2014).

Ouyang, L. et al. Programmed cell death pathways in cancer: A review of apoptosis, autophagy and programmed necrosis. *Cell Proliferation* **45**, 487–498 (2012).

Papandreou, I. et al. Hypoxia signals autophagy in tumor cells via AMPK activity, independent of HIF-1, BNIP3, and BNIP3L. *Cell death and differentiation*, **15**, 1572–1581 (2008).

Parkin, D.M. et al. Global cancer statistics. *Journal of Cancer Research and Clinical Oncology* **55**, 74–108 (2002).

Pieniążek, a et al. Oxidative stress induced in rat liver by anticancer drugs doxorubicin, paclitaxel and docetaxel. *Advances in medical sciences* **58**, 104–11 (2013).

Prakash, O. et al. Anticancer Potential of Plants and Natural Products: A Review. *American Journal of Pharmacological Sciences* **1**, 104–115 (2013).

Qu, X. et al. Promotion of tumorigenesis by heterozygous disruption of the beclin 1 autophagy gene. *Journal of Clinical Investigation* **112,** 1809–1820 (2003).

Ravikumar, B. et al. Regulation of mammalian autophagy in physiology and pathophysiology. *Physiological reviews* **90**, 1383–1435 (2010).

Reichardt, P. et al. Exatecan in pretreated adult patients with advanced soft tissue sarcoma: Results of a phase II - Study of the EORTC Soft Tissue and Bone Sarcoma Group. *European Journal of Cancer* **43**, 1017–1022 (2007).

Rosenthal, P.J. & Meshnickb, S.R. Hemoglobin catabolism and iron utilization by malaria parasite. *Molecular and Biochemical Parasitology* **83,**

131-139 (1996).

Rubinsztein, D.C. et al. In search of an “autophagomometer.” *Autophagy* **5**, 585–589 (2009).

Sarkar, S. Regulation of autophagy by mTOR-dependent and mTOR-independent pathways: autophagy dysfunction in neurodegenerative diseases and therapeutic application of autophagy enhancers. *Biochemical Society Transactions* **41**, 103–1130 (2013).

Sarvothaman, S. et al. Apoptosis: role in myeloid cell development. *Blood research* **50**, 73–79 (2015).

Shang, L. & Wang, X. AMPK and mTOR coordinate the regulation of Ulk1 and mammalian autophagy initiation. *Autophagy* **7**, 924–926 (2011).

Shen, S., Zhang, Y., Wang, Z., et al. Bufalin induces the interplay between apoptosis and autophagy in glioma cells through endoplasmic reticulum stress. *International journal of biological sciences* **10**, 212–224 (2014).

Shen, S., Zhang, Y., Zhang, R., et al. Ursolic acid induces autophagy in U87MG cells via ROS-dependent endoplasmic reticulum stress. *Chemico-biological interactions* **218**, 28–41 (2014).

Shimada Yutaka, M.D. Characterization of the 21 newly established Esophageal cancer cell lines. *Cancer* **69,** 2 (1992).

Shimizu, S. et al. Role of Bcl-2 family proteins in a non-apoptotic programmed cell death dependent on autophagy genes. *Nature cell biology* **6**, 1221–1228 (2004).

Shimizu, S., Eguchi, Y. & Kamiike, W. Induction of Apoptosis as well as Necrosis by Hypoxia and Predominant Prevention of Apoptosis by Bcl-2 and Bcl-X L. *Cancer Research* 56, 2161–2166 (1996) .

Shimodaira, Y. et al. Modulation of endoplasmic reticulum (ER) stress-induced autophagy by C/EBP homologous protein (CHOP) and inositol-requiring enzyme 1α (IRE1α) in human colon cancer cells. *Biochemical and biophysical research communications* **445**, 524–533 (2014).

Shunmoogan- Gounden, N 2014. An investigation into the molecular mechanisms induced by derivatives of natural products in esophageal cance. PhD thesis, The University of Cape Town, 23 January 2015, open.uct.ac.za/ handle/11427/7909.

Siegel, R. et al. Cancer Treatment and Survivorship Statistics , 2012. *CA: Cancer Journal for Clinicians* **62**, 220-241(2012).

Siegel, R., Miller, K. & Jemal, A. Cancer statistics , 2015 . *CA: A Cancer Journal for Clinicians* **65**, 29 (2015).

Singh, N.P. & LAI, H.C. Artemisinin Induces Apoptosis in Human Cancer Cells. *Anticancer Research* **24**, 2277–2280 (2004).

Srivastava, V. et al. Plant-based anticancer molecules: A chemical and biological profile of some important leads. *Bioorganic and Medicinal Chemistry* **13**, 5892–5908 (2005).

Stockwin, L.H. et al. Artemisinin dimer anti-cancer activity correlates with heme- catalyzed ROS generation and ER stress induction. *International journal of cancer. Journal international du cancer* **125**, 1266 (2009).

Stokoe, D. et al. Dual Role of Phosphatidylinositol-3,4,5-triphosphate in the Activation of Protein Kinase B. *Science* **277**, 567–570 (1997).

Su, M., Mei, Y. & Sinha, S. Role of the crosstalk between autophagy and apoptosis in cancer. *Journal of Oncology*, 2013 (2013).

Sun, Q. et al. Identification of Barkor as a mammalian autophagy-specific factor for Beclin 1 and class III phosphatidylinositol 3-kinase. *Proceedings of the National Academy of Sciences of the United States of America* **105**, 19211–19216 (2008) .

Sun, Y. & Peng, Z.-L. Programmed cell death and cancer. *Postgraduate medical journal* **85**, 134–140 (2009).

Suzuki, K. et al. Hierarchy of Atg proteins in pre-autophagosomal structure organization. *Genes to Cells* **12**, 209–218 (2007)

Suzuki, K. et al. The pre-autophagosomal structure organized by concerted functions of APG genes is essential for autophagosome formation. *EMBO Journal* **20**, 5971–5981 (2001).

Szegezdi, E. et al. Mediators of endoplasmic reticulum stress-induced apoptosis. *EMBO reports* **7**, 880–885 (2006).

Takahashi, Y. et al. Loss of Bif-1 Suppresses Bax / Bak Conformational Change and Mitochondrial Apoptosis. *Molecular and Cellular Biology* **25**, 9369–9382 (2005).

Tan, M.L. et al. Programmed cell death pathways and current antitumor targets. *Pharmaceutical Research* **26**, 1547–1560 (2009).

Teiten, M.H., Dicato, M. & Diederich, M. Hybrid curcumin compounds: A new strategy for cancer treatment. *Molecules* **19**, 20839–20863 (2014).

Thoreen, C.C. et al. An ATP-competitive mammalian target of rapamycin inhibitor reveals rapamycin-resistant functions of mTORC1. *Journal of Biological Chemistry* **284**, 8023–8032 (2009).

Tobin, G., Kalupahana, R. & Kulka, M. Plant Based Natural Products and Breast Cancer : Considering Multi-Faceted Disease Aspects , Past Successes , and Promising Future Interventions. 30–40 (2012).

Wang, C.-W. & Klionsky, D.J. The Molecular Mechanism of Autophagy. *Molecular Medicine* **9**, 65–76 (2003).

White, E. & DiPaola, R.S. The double-edged sword of autophagy modulation in cancer. *Clinical Cancer Research* **15**, 5308–5316 (2009).

Wong, V.K.W. et al. Saikosaponin-d, a novel SERCA inhibitor, induces autophagic cell death in apoptosis-defective cells. *Cell death & disease* **4**, p.e720 (2013).
Wu, W., Liu, P. & Li, J. Necroptosis: An emerging form of programmed cell death. *Critical Reviews in Oncology/Hematology* **82**, 249–258 (2012).

Wullschleger, S., Loewith, R. & Hall, M.N. TOR signaling in growth and metabolism. *Cell* **124**, 471–484 (2006).

Xu, Q. et al. Artesunate inhibits growth and induces apoptosis in human osteosarcoma HOS cell line in vitro and in vivo. *Journal of Zhejiang* **12**, 247–255 (2011).

Yang, Z. & Klionsky, D.J. Mammalian autophagy: Core molecular machinery and signaling regulation. *Current Opinion in Cell Biology* **22**, 124–131 (2010).

Yde, C.W. & Issinger, O.-G. Enhancing cisplatin sensitivity in MCF-7 human breast cancer cells by down-regulation of Bcl-2 and cyclin D1. *International journal of oncology* **29**, 1397–1404 (2006).

Yorimitsu, T. et al. Endoplasmic reticulum stress triggers autophagy. *Journal of Biological Chemistry* **281**, 30299–30304 (2006).

Yorimitsu, T. & Klionsky, D.J. Eating the endoplasmic reticulum: quality control by autophagy. *Trends in Cell Biology* **17**, 279–285 (2007).

Younce, C.W. & Kolattukudy, P.E. MCP-1 causes cardiomyoblast death via autophagy resulting from ER stress caused by oxidative stress generated by inducing a novel zinc-finger protein, MCPIP. *The Biochemical journal*, **426**, 43–53 (2010).

Yu, L. et al. Autophagic programmed cell death by selective catalase degradation. *Proceedings of the National Academy of Sciences of the United States of America* **103**, 4952–4957 (2006).

Yue-Zhong Shu. Recent natural products based drug development: A pharmaceutical industry perpesctive. *Journal of natural products* **61**, 1053–1071 (1998).

Yue, Z. et al. Embryonic Development , Is a Haploinsufficient Tumor

Suppressor. *Pnas* **100**, (2003).

Zapata, J.M. et al. A Diverse Family of Proteins Containing Tumor Necrosis Factor Receptor-associated Factor Domains. *Journal of Biological Chemistry*, **276**, 24242–24252 (2001) .

Zeng, X. & Kinsella, T.J. Impact of Autophagy on Chemotherapy and Radiotherapy Mediated Tumor Cytotoxicity: “To Live or not to Live”. *Frontiers in oncology* **1**, 30 (2011) .

Zhang, S. & Gerhard, G.S. Heme mediates cytotoxicity from artemisinin and serves as a general anti-proliferation target. *PLoS ONE* **4**, (2009).

Zhang, X. et al. Why should autophagic flux be assessed? *Acta pharmacologica Sinica* **34**, 595–599 (2013).

Zhou, C. et al. Artesunate induces apoptosis via a Bak-mediated caspase-independent intrinsic pathway in human lung adenocarcinoma cells. *Journal of Cellular Physiology* **227**, 3778–3786 (2012).

APPENDIX A: SOLUTIONS

Protein solutions

1M Tris pH 6.8

60.5 g Tris
300 ml dH_2O
pH with concentrated HCl to pH 6.8
Volume made up to 500 ml with dH_2O

1 M Tris pH 8.8

60.5 g Tris
300 ml dH_2O
pH with concentrated HCl to pH 8.8
Volume made up to 500 ml with dH_2O

RIPA Buffer

150 mM NaCl
1% Triton x-100
0.5% Sodium Deoxycholate
0.1% SDS
50 mM Tris, pH 8.0

10 X PBS

40 g NaCl
1 g KCl
1 g KH_2PO_4
3.82 g $Na_2HPO4.2H_2O$
up to 500 ml dH_2O

Western Blot solutions

10% stacking gel

2.75 ml dH_2O
3.75 ml 1M Tris PH 8.8
100 µl 10% SDS
3.35 ml 30% acrylamide
200 µl 10% APS
20 µl TEMED

Resolving gel

3.65 ml dH_20
625 µl 1M Tris, pH 6.8
50 µl 10% SDS
650 µl 30% acrylamide
60 µl 10% APS
6 µl TEMED

15% stacking gel

2.3 ml dH_20
1.67 ml 1M Tris PH 8.8
100 µl 10% SDS
5 ml 30% acrylamide
100 µl 10% APS
10 µl TEMED

Resolving gel

3 ml dH_20
2.5 ml 1M Tris, pH 6.8
50 µl 10% SDS
670 µl 30% acrylamide
50 µl 10% APS
5 µl TEMED

10 X Running Buffer

20 g Glycine
31.6 g Tris
50 ml 10% SDS
Up to 500 ml with dH_2O

1 X Running Buffer

100 ml 10 X running buffer
900 ml dH_2O

10 X Transfer Buffer

72 g Glycine
19 g Tris
Up to 500 ml with dH_2O

1 X Transfer Buffer

200 ml Isopropanol
100 ml 10 X Transfer Buffer
700 ml dH_2O

6 X loading dye

0.8 ml Glycerol
0.1 ml Bromophenol Blue
0.5 ml Tris pH 6.8
0.6 ml 20 % SDS
10 µl 100% β-mercaptoethanol

10 X TBS

24.23 ml Trizma (HCl) or Tris
80.06 g NaCl

Mix in 800 ml dH_2O

pH with concentrated HCl to pH 7.6

Volume made up to 1000 ml dH_2O

1 X TBST

100 ml 10 X TBS

900 ml dH_2O

1 ml Tween-20

5 % milk powder

5 g milk

100 ml TBST

MTT and drugs treatment assays

MTT (100mg/20ml)

100 mg MTT
20 ml 1X PBS
Vortex and incubate for 15 min at 37˚C

Filter through a 0.2 µm filter

Wrap in foil and store in the dark at 4˚C for up to 1 month

Solubilisation reagent

25 g SLS

Up to 250 ml with dH_2O

76.6 µl concentrated HCl

RNA isolation and Electrophoresis

DEPC-treatment

0.1 % DEPC in distilled dH_2O

Stir for one hour at room temperature

Incubate overnight at room temperature

Autoclave

RNA gel

0.75 g agarose
42 ml dH_2O
Heat and allow to cool
Add 5 ml 10 X MOPS
2.7 ml Formahaldehyde

10 X MOPS

41.86 g MOPS
16.6 ml 3 M NaAcetate
20 ml 0.5 M EDTA (pH 7.0)
Adjust to 1L (DEPC-H_2O)
Cover in foil and store a 4°C
Dilute to 1X MOPS as needed

2 X RNA loading Dye

0.72 ml Formamide
0.16 ml 10 X MOPS
0.26 ml Formaldehyde
0.04 ml dH_2O
0.1 ml glycerol
0.2 ml bromophenol blue (0.25 % Depc-dH_2O)
50 µg/ml ethiduium bromide
Store at - 20˚ C

DNA electrophoresis

10 X TBE

108 g TRIS
55 g Boric acid
7.4 g EDTA
Made up to 1000 ml dH_2O

2 % Agarose gel

2 g Agarose

10 ml 1 X TBE

90 ml dH_2O

2 µl ethidium bromide

APPENDIX B

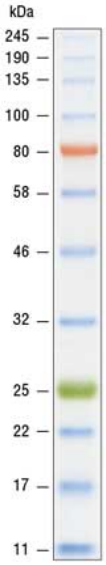

Figure 1: SDS-PAGE prestain protein marker (NEB, P7712).

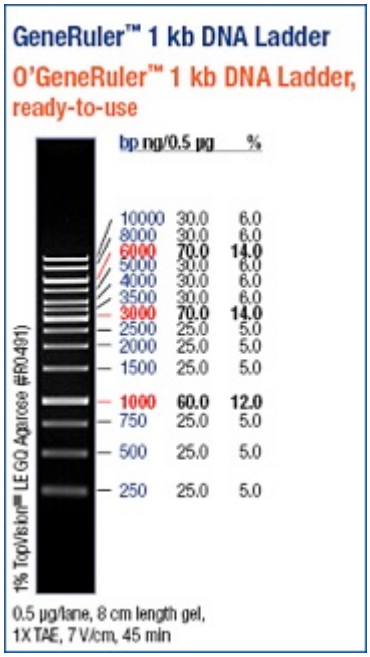

Figure 2: O' Genruler 1kb DNA for use a ladder